Biodiversity and Conservation (2026) 35:155
https://doi.org/10.1007/s10531-026-03345-5

ORIGINAL RESEARCH

From terrestrialisation to disturbance: long-term trajectories of a fen ecosystem and its conservation implications in the Xistral Mountains, NW Iberia

Álvaro Hernando Bartolomé[1] · **Álvaro Moreno Martín**[1] · **Rosina Magaña Ugarte**[1] · **Saúl Manzano**[2,3,4] · **Antonio Martínez Cortizas**[5,6] · **Lourdes López-Merino**[1]

Received: 6 November 2025 / Revised: 26 March 2026 / Accepted: 1 April 2026

Abstract

Peatlands in north-west Iberia are globally important carbon reservoirs, yet their fen communities remain less well understood than those of bogs. Here, we present a multiproxy study of a ~11,100 cal. yr BP peat sequence cored at the Toxiza fen (TOX, Xistral Mountains, Galicia). Our analyses of palynology, rarefaction, charcoal, elemental composition and CIELab colour identify three main ecological phases. First, early Holocene mire initiation through terrestrialisation: wet meadows progressively replaced by a transitional fen at ~10,350 cal. yr BP, and subsequently by a *Sphagnum*-rich fen. Second, the mire experienced a prolonged phase of hydrological stability during the Holocene Climatic Optimum, characterised by *Sphagnum*-rich vegetation, high organic-matter content and sustained peat accumulation. Third, late Holocene increasing disturbance, including catchment erosion (~4900-4200 cal. yr BP) and fire-intense phases leading to an Ericaceae-rich fen; with *Sphagnum* partially recovered in reduced-burning intervals. Phases of ecological transition (i.e., early Holocene terrestrialisation and late Holocene disturbance) showed higher pollen richness, whereas comparatively stable values were found during the mid-Holocene, reflecting long-term ecosystem stability. Comparisons with nearby ombrotrophic mires highlight the importance of hydrological setting (minerotrophy vs. ombrotrophy) in shaping peatland vegetation trajectories under similar climatic forcing. Today the fen shows clear signs of degradation, including fire activity, sediment inputs and afforestation pressure, with no clear *Sphagnum* recovery. The TOX record, therefore, provides a process-based reference baseline for conservation where the mid-Holocene *Sphagnum*-rich phase represents a benchmark of hydrological stability and minimal disturbance, offering a framework for understanding biodiversity change and for guiding restoration of minerotrophic peatlands under ongoing environmental change.

Keywords Palynology · *Sphagnum* · Fire history · Minerotrophy · Holocene · Peatland restoration

---

Communicated by Daniel Sanchez Mata.

Extended author information available on the last page of the article

Introduction

Peatlands cover ~3% of the Earth's land surface yet store more carbon than the world's forests combined (Yu et al. 2010; Yu 2012). This disproportionate role reflects the slow accumulation of partially decomposed plant material (peat) under persistently waterlogged, anoxic conditions that strongly limit microbial decay (Rydin and Jeglum 2013). Beyond carbon storage, peatlands regulate catchment hydrology, influence regional biogeochemical cycles, and support specialised biodiversity. In Europe, many peatland habitats are recognised as priority conservation ecosystems under the EU Habitats Directive (92/43/EEC) and are protected through the Natura 2000 network (European Commission 2013). Despite this protection, peatlands remain highly vulnerable to several perturbations such as hydrological alteration, catchment disturbance, fire, and pollution, all of which can disrupt peat-forming vegetation and compromise ecosystem functioning (Mursyid et al. 2025).

In north-west Iberia, particularly Galicia, an oceanic climate with high and relatively evenly distributed precipitation favours peat formation and supports one of Europe's densest concentrations of active Atlantic mires (Martínez Cortizas et al. 1999a; Martínez Cortizas and García Rodeja Gayoso 2001; Pontevedra-Pombal et al. 2006; Silva-Sánchez et al. 2023). In particular, the Xistral Mountains (Septentrional Ranges) constitute a key peatland region in Galicia, supporting extensive peat cover and representing one of the southernmost Atlantic blanket-bog refuges in Europe. Peat-forming environments include organic-rich mineral soils, ombrotrophic peatlands (bogs) and minerotrophic peatlands (fens) (Martínez Cortizas and García Rodeja Gayoso 2001; Pontevedra-Pombal et al. 2006; Silva-Sánchez et al. 2023). These peatlands, included in the Natura 2000 network (Site ES1120003), have been investigated intensively, particularly through bog records. For instance, geochemical studies in the Xistral Mountains document long-term changes in peat functioning (including shifts from sediment to fen to bog) and changes in mineral matter and metal fluxes linked to climatic variability and atmospheric pollution (Martínez Cortizas et al. 1997a, b, 1999b, 2002, 2005, 2012, 2020; Kylander et al. 2005; Pontevedra-Pombal et al. 2012, 2013, 2019). Similarly, Holocene pollen sequences describe broad landscape trends in the area – from early post-glacial forest expansion to late Holocene anthropogenic opening – while also recording shorter climatic perturbations such as the 8.2 cal. ka BP event (Ramil-Rego et al. 1994, 1998; Martínez Cortizas et al. 2005, 2009, 2020; Muñoz Sobrino et al. 2005; Mighall et al. 2006, 2023; Stefanini et al. 2018).

Nevertheless, conservation decisions often require information at the habitat and plant-community scale, because peatland integrity is ultimately maintained by the taxa that build peat and sustain mire functioning. In the Xistral Mountains, mire-scale reconstructions remain comparatively limited compared with upland, landscape-scale reconstructions, especially for minerotrophic systems. Among the few existing studies focused on the Xistral Mountain peatland vegetation, organic molecular markers applied to modern mire plants and an 8000-year-old peat record from the Penido Vello (PVO) bog identified a fen-to-bog transition ~6500-6200 years ago, but decomposition differences between the fen and bog phases constrained detailed community assignments for the fen interval (Schellekens et al. 2011). Macrofossil work refined vegetation histories in several bogs (Castro 2017; Souto 2018), including an autogenous fen-to-bog transition at Chao de Veiga Mol (CVM), mid- to late Holocene wet-dry cycles at Pena da Cadela (PDC) (Castro et al. 2015), and macro-remain keys highlighting *Erica mackaiana*, *Molinia caerulea*, *Eriophorum angustifolium* and *Carex* spp. as main components of key peat-forming assemblages (Souto et al. 2016, 2017). Further multi-proxy records at Tremoal do Pedrido (TPD) bog and high-resolution macroremain work at CVM have resolved late Holocene palaeohydrological variability and events such as the Medieval Climate Anomaly and the Little Ice Age (Stefanini et al. 2018; Castro et al. 2020). Yet, most reconstructions in the Xistral Mountains still derive from rain-fed bogs, and fen-specific ecological trajectories and catchment controls remain underrepresented.

This knowledge gap is critical because fens are hydrologically coupled to their catchments and can be particularly sensitive to changes in sediment delivery, erosion, fire regime and land use (Silva-Sánchez et al. 2023). From a biodiversity and conservation viewpoint, this coupling complicates management: site-level protection may be insufficient if off-site pressures shift minerotrophic conditions and alter plant community composition. Thus, long-term records that integrate vegetation indicators with disturbance and geochemical proxies are required to define reference conditions, identify thresholds of change, and support realistic management targets for fen habitats. Currently, this knowledge gap limits our ability to define conservation targets based on long-term ecosystem behaviour, particularly for minerotrophic peatlands that are highly sensitive to catchment-scale disturbances.

In this study we analyse a 151-cm peat core (TOX) from the Toxiza fen in the Xistral Mountains using pollen and non-pollen palynomorph (NPP) analyses, together with CHNS elemental data, charcoal, CIELab colorimetry and an AMS-based Bayesian chronology. Our objectives are:

i. to identify the palynological assemblages that characterise peatland communities through time;
ii. to link local mire dynamics with regional environmental drivers; and
iii. to identify the processes controlling biodiversity and ecosystem resilience in minerotrophic peatlands.

By explicitly addressing a minerotrophic system that is hydrologically coupled to its catchment, this study contributes to defining reference conditions for fen habitats in the Xistral Mountains. The long-term record helps identify periods of ecological stability and thresholds of change, providing a framework for habitat monitoring and for setting conservation targets under ongoing climatic and anthropogenic pressures.

Materials and methods

Site description and peat coring

The Toxiza fen (43° 27’ 12.28” N; 7° 31’ 29,92” W; 709 m a.s.l.) is a minerogenic valley mire in the Xistral Mountains (Lugo, Galicia, Spain; Fig. 1). As the western extension of the Cantabrian Mountains, the range reaches elevations of ~1000 m a.s.l. and intercepts moist Atlantic air masses (Fraga et al. 2008). Climate is Atlantic European, ranging from very to extremely humid; annual rainfall ~1400-1800 mm; mean annual temperatures ~ 7-10°C with low to moderate seasonality (Martínez Cortizas et al. 1999a; Martínez Cortizas and

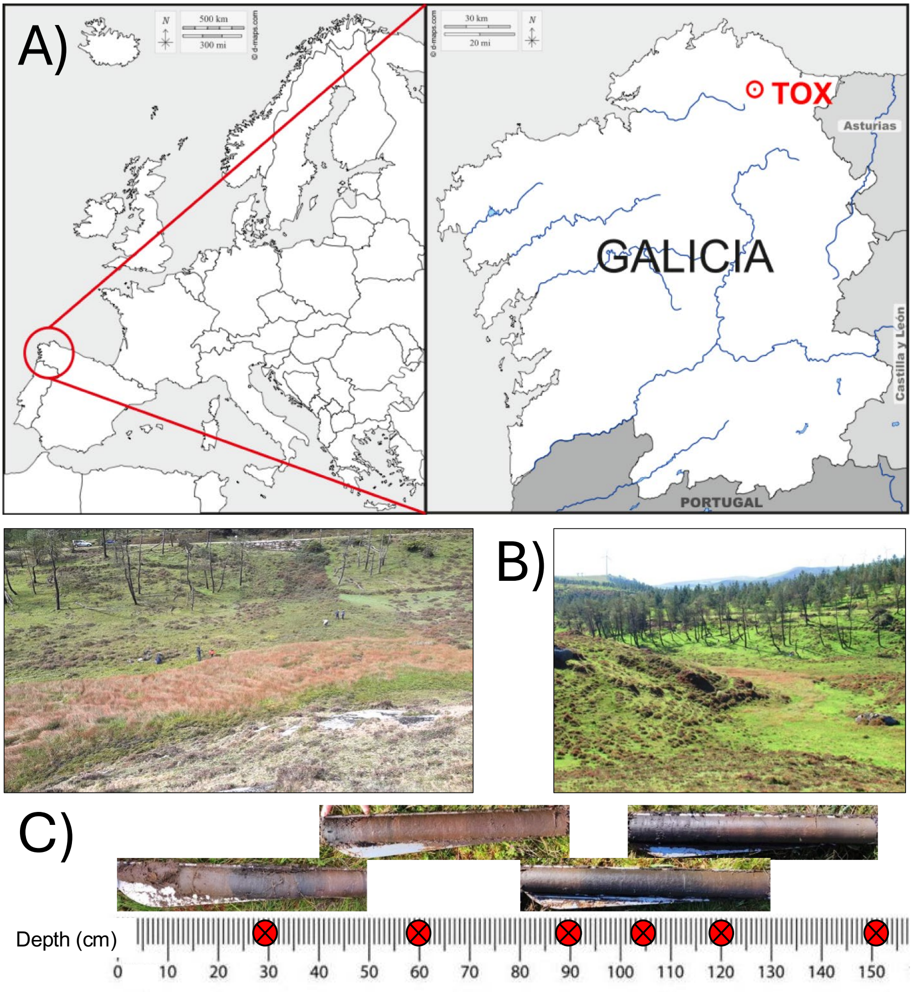

Fig. 1 **A**) Location of the Toxiza fen within the Xistral Mountains of Galicia (Spain). **B**) Photographs of the Toxiza fen illustrating its valley-mire characteristics (left: September 2021, photo by Antonio Martínez Cortizas; right: September 2022, photo by Álvaro Hernando Bartolomé). **C**) Core sections sampled at the Toxiza fen (TOX) using a Russian corer. Total peat depth of the core sequence was 151 cm. Symbols denote depths at which radiocarbon dates were obtained

García Rodeja Gayoso 2001). Geology is dominated by Precambrian quartzite formations (Pontevedra-Pombal et al. 2006).

The Toxiza fen forms part of a heterogeneous Atlantic mountain landscape where peatlands occur as a mosaic of bogs and minerotrophic valley mires surrounded by heathlands, wet grasslands and managed forest stands. Present-day vegetation patterns reflect strong oceanic influence but are also shaped by long-standing grazing, drainage for agriculture and, more recently, commercial afforestation and wind farms (Silva-Sánchez et al. 2023). These pressures may alter catchment hydrology and sediment delivery, potentially affecting the ecological functioning of minerotrophic systems such as fens, which are tightly coupled to their drainage basins. The fen occupies a small ~ 0.33-ha catchment, where peat-forming vegetation depends on drainage from surrounding slopes. Vegetation is adapted to acidic and oligotrophic conditions, and is dominated by vascular plants, including sedges (*Eriophorum angustifolium*, *Eleocharis multicaulis*, *Carex demissa*, *C. durieui*, *C. echinata*, *C. panicea*), grasses (*Molinia caerulea*, *Agrostis canina*), and rushes (*Juncus bulbosus*), along with Mackay's heath (*Erica mackaiana*). Compared to boreal mires, mosses play a less dominant role in NW Spain peatlands. However, *Sphagnum* spp. is relatively abundant in the Xistral Mountains mires, including the Toxiza fen, although its presence is more prominent in bogs.

A floristic list of the plant species recorded in the Toxiza fen in autumn 2021 and spring 2022 is provided in Table 1, together with their palynological equivalents in the TOX palynological diagram. The table functions as a site-specific vegetation–pollen comparison and is used as a framework for interpreting Holocene assemblages in terms of local fen vegetation and ecosystem functioning. A total of 32 vascular plants were recorded, in addition to *Sphagnum* spp. and other unidentified mosses (Bryopsida). Vascular plant identification and nomenclature follow Flora iberica (http://www.floraiberica.org/), yet family rank systema tics have been updated to APGIV (The Angiosperm Phylogeny Group et al. 2016). Plant identifications are supported by vouchers collected by and deposited in the LEB Herbarium (vouchers LEB127609-LEB127637; collection numbers PALEOFUN1-29; Supplementary Herbarium vouchers).

In autumn 2022 a 151-cm long core (TOX) was obtained with a Russian corer (50-cm chamber, 5-cm diameter) using two parallel boreholes (TOX-A, TOX-B) with ~10 cm overlapping sections. The core sections were stored in PVC tubes, protected with plastic cling wrap, and kept refrigerated (4 °C) prior to analyses. The core stratigraphy comprised six units: Unit I (151-140.5 cm): organic-rich mineral sediment; Unit II (140.5-123): brown peat; Unit III (123-94 cm): black peat; Unit IV (94-40 cm): brown peat with decomposed plant remains and a sand-rich layer at 94-84 cm; Unit V (40-20.5 cm): stratified brown-black peat with charcoal fragments; and Unit VI (20.5-0 cm): brown peat with mineral input, with the uppermost centimetres corresponding to living vegetation (Fig. 1).

Radiocarbon dating and chronological model

Six samples (the basal organic-rich sediment and five peat samples) were radiocarbon dated by Accelerator Mass Spectrometry (AMS) at Beta Analytic Inc. (Miami, FL, USA). All samples were pre-treated using a standard acid-alkaline-acid (AAA) protocol to isolate bulk organic matter prior to measurement. Radiocarbon ages were calibrated using the IntCal20 calibration curve (Reimer et al. 2020; Table 2).

An age-depth model was constructed within a Bayesian framework by integrating the calibrated radiocarbon dates with independent chronological constrains. These included the well-documented onset of *Pinus pinaster* afforestation in the Xistral Mountains in 1955 AD (±10 years) (Díaz Varela et al. 1997) at 18.5 cm, and the coring year assigned to the uppermost sample (±10 years). The model was generated using the software *Bacon* 2.3 (Blaauw and Christen 2011). According to the model, the TOX core spans the last ~11,100 years (Fig. 2) with no evidence of age reversals and uninterrupted sediment/peat accumulation. However, accumulation rates appear lower between ~8700 and 4400 cal. yr BP relative to earlier and later intervals.

Physicochemical analyses

Samples at 1-cm intervals were split: one half refrigerated (4 °C), the other oven-dried (30 °C). From the oven-dried samples, seventy-four (mainly 2-cm spacing, adjusted around the sand-rich layer) were subjected to CHNS elemental and colorimetric analyses. Before the analyses, samples were milled using a Retsch MM 400 automated mixer mill at the PalaeoChange Lab, Universidad Complutense de Madrid (UCM).

Carbon (C), nitrogen (N), and sulphur (S) contents were measured by complete combustion in a LECO CHNS-932 Elemental Analyzer at the Elemental Microanalysis Unit of the UCM Chemical Technologies Research Support Centre. The carbon to nitrogen ratio (C/N) was calculated as a proxy for the degree of organic matter decomposition. To complement the stratigraphic characterisation of the core, colour parameters were determined using a Konica-Minolta CR-5 colorimeter for solids. Measurements were conducted in the CIELab colour space at the EcoPast research group facilities of the Universidade de Santiago de Compostela. The output included quantitative values for lightness (L*), and colour coordinates (a* and b*). These parameters are used to describe and quantify the colour of an object or surface. L* represents lightness, ranging from black (0) to white (100), while a* and b* represent the red/green and blue/yellow components, respectively.

Palynological analysis

A total of 39 samples (~1 cm^3; ~4 cm spacing) were processed at the Quaternary Palynology Lab of the Universidad de León. Standard chemical treatments were applied: 10% hydrochloric acid (HCl) to remove carbonates, 20% sodium hydroxide (NaOH) to eliminate humic substances, and 48% hydrofluoric acid (HF) to dissolve silicates. Two to three *Lycopodium clavatum* spore tablets (Batch no. 3862) were added per sample to calculate concentrations (Stockmarr 1971). The residues were mounted on slides with glycerol for microscopic analysis.

Palynological identification and counting were carried out at the PalaeoChange Lab (UCM) using a Leica DM2000 LED light microscope at ×400 magnification and ×1000 with immersion oil for finer identifications. Reference materials included in-house reference collections and manuals (Faegri et al. 1989; Moore et al. 1991; Reille 1992, 1995, 1998). Most taxa were identified following Moore et al. (1991), while specific taxa were identified using specialist keys: *Plantago* pollen types (Clarke and Jones 1977), Oleaceae genera (Renault-Miskovsky et al. 1976), *Pinus* pollen types (Carrión et al. 2000), *Urtica dioica* t. (Punt and Malotaux 1984), and *Cerealia* t. (López Sáez and López Merino 2005). NPP identification followed van Geel in Smol et al. (2002) and Marret et al. (2021). Lactuceae is named Cichorioideae in this study. Pollen type nomenclature aligns with the standards in Joosten and de Klerk (2002).

The pollen sum per sample comprised approximately 400 grains (minimum = 394; average = 527; median = 504), excluding spores, fungal and algal remains, other NPP and reworked pollen. Pollen percentages were calculated based on this pollen sum, whereas NPP and reworked percentages were calculated relative to the palynological sum (pollen + RW + NPP).

Table 1 Modern vegetation recorded in the Toxiza fen (Xistral Mountains, Galicia, Spain) and its palynological equivalents in the TOX diagram

Division/Clade	Class/Family	Taxon recorded in the fen	Braun-Blanquet scale	Palynological equivalent in TOX	Detected in TOX	Pollination	Ecological setting in the fen	Note for interpretation
Bryophyta	Sphagnopsida	*Sphagnum*	3	*Sphagnum*	Yes	Spore-producing	Mire-forming moss	Local peat-forming taxon
	Bryopsida	Bryopsida	2	Bryophyta spores	Yes	Spore-producing	Ground mosses	Low taxonomic resolution
Monocots	Cyperaceae	*Carex demissa*	2	Cyperaceae undiff.	Yes	Anemophilous	Fen graminoid	Peat-forming component
		Carex durieui	2					
		Carex echinata	2					
		Carex panicea	1					
		Eleocharis multicaulis	3					
		Eriophorum angustifolium	2					
	Juncaceae	*Juncus acutiflorus*	+	Juncaceae	No	Anemophilous	Wet microsites	Not detected in TOX
		Juncus articulatus	+					
		Juncus bulbosus	4					
		Juncus bufonius	+					
	Poaceae	*Agrostis canina*	1	Poaceae undiff.	Yes	Anemophilous	Wet grassland	Shared pollen type
		Molinia caerulea	3				Fen margin / fen–heath transition	Shared pollen type; transitional taxon
	Potamogetonaceae	*Potamogeton polygonifolius*	2	Potamogetonaceae	Yes	Anemo/hydrophilous	Shallow-water aquatic habitat	Hydro-hygrophilous indicator
	Nartheciaceae	*Narthecium ossifragum*	+	*Narthecium*	No	Entomophilous	Oligotrophic acidic fen / fen–heath transition	Not detected in TOX

Table 1 (continued)

Division/Clade	Class/Family	Taxon recorded in the fen	Braun-Blanquet scale	Palynological equivalent in TOX	Detected in TOX	Pollination	Ecological setting in the fen	Note for interpretation
Eudicots	Apiaceae	*Carum verticillatum*	1	Apiaceae	Yes	Entomophilous	Wet fen / wet grassland	Broad pollen type
	Araliaceae	*Hydrocotile vulgaris*	+	*Hydrocotile*	No	Entomophilous	Wet surfaces / flushes	Not detected in TOX
	Asteraceae	*Arnica montana*	+	*Aster* t.	Yes	Entomophilous	Open microsites within/around fen	Broad pollen type
		Thrincia saxatilis	+	Cichorioideae	Yes	Entomophilous	Open disturbed microsites	Broad pollen type
	Ericaceae	*Calluna vulgaris*	+	*Calluna vulgaris*	Yes	Anemophilous	Heathland component	Disturbance / drier conditions indicator
		Erica mackaiana	2	Ericaceae undiff.	Yes	Entomophilous	Fen–heath transition	Shared pollen type
	Primulaceae	*Anagallis tenella*	1	*Anagallis tenella* t.	No	Entomophilous	Wet microhabitats	Not detected in TOX
	Gentianaceae	*Gentiana pneumonanthe*	+	*Gentiana pneumonanthe* t.	Yes?	Entomophilous	Oligotrophic fen	Low-confidence detection
	Lentibulariaceae	*Utricularia*	+	*Utricularia*	No	Self-pollinated	Aquatic microhabitats	Not detected in TOX
	Orobanchaceae	*Pedicularis sylvatica*	+	*Pedicularis palustris* t.	Yes	Entomophilous	Wet grassland / fen margin	Type-level identification only
	Hypericaceae	*Hypericum elodes*	2	*Hypericum*	No	Entomophilous	Wet acidic fen	Not detected in TOX
	Violaceae	*Viola palustris*	1	*Viola palustris* t.	No	Entomophilous	Wet soils / fen margin	Not detected in TOX
	Celastraceae	*Parnassia palustris*	+	*Parnassia palustris*	Yes	Entomophilous	Oligotrophic acidic fen	Useful local fen indicator
	Fabaceae	*Lotus pedunculatus*	+	*Lotus* t.	Yes	Entomophilous	Wet grassland	Type-level identification only
	Rosaceae	*Potentilla erecta*	2	*Potentilla* t.	Yes	Entomophilous	Fen margin / transition	Type-level identification only
	Droseraceae	*Drosera intermedia*	+	*Drosera intermedia* t.	Yes	Entomophilous	Wet oligotrophic hollows	Hydro-hygrophilous / oligotrophic indicator
		Drosera rotundifolia	+	*Drosera rotundifolia* t.	No	Entomophilous	Wet oligotrophic microsites	Not detected in TOX
	Ranunculaceae	*Ranunculus flammula*	1	*Ranunculus acris* t.	Yes	Entomophilous	Shallow water / wet microsites	Type-level identification only

The table functions as a site-specific vegetation–pollen comparison based on the present-day fen vegetation. “Detected in TOX” refers to the presence of the corresponding pollen/spore type in the fossil palynological diagram, not to its abundance in the modern vegetation survey. The additional columns “Ecological setting in the fen” and “Note for interpretation” are included to facilitate interpretation of pollen assemblages in terms of local vegetation dynamics and ecosystem functioning

Microcharcoal and macrocharcoal analyses

Microcharcoal analysis was performed on the same 39 palynological slides. Microcharcoal particles >10 µm were identified based on their opaque black coloration and angular morphology, exhibiting a distinctive bluish hue along their edges under transmitted light (Turner et al. 2008). Identification and counting were carried out using a Leica DM2000 LED light microscope at ×400 magnification. A minimum of 200 particles (including both microcharcoal and *Lycopodium* spores) were counted per sample, following established protocols (Carcaillet et al. 2001; Finsinger et al. 2008).

Macrocharcoal analysis was conducted on ~1 cm^3 of all 151 samples at the UCM Palaeo-Change Lab. Samples were treated with 10% potassium hydroxide (KOH) and gently agitated on a mixer for 24 hours. After discarding the supernatant, samples were treated with 5% hydrogen peroxide (H_2O_2) for an additional 24 hours to bleach organic matter while preserving charcoal fragments. The resulting suspension was passed through a 150 µm mesh sieve, and the retained material was stored in distilled water until charcoal particles were counted under a stereomicroscope at ×10–15 magnification (Stevenson and Haberle 2018).

Microcharcoal and macrocharcoal data were converted to charcoal accumulation rates (named microcharcoal influx and CHAR respectively), expressed as number of particles per square centimetre per year (particles cm^{-2} yr^{-1}).

Numerical methods

To characterise assemblages, we performed a principal components analysis (PCA) on the transposed data matrix (PCAtr: samples as variables; taxa as cases). The data were Z-scored, and PCA was conducted on the correlation matrix with varimax rotation using IBM SPSS Statistics 28.0.1.1, following previous applications of this approach (López-Merino et al. 2012, 2016, 2023; Horák-Terra et al. 2015; Mighall et al. 2023). Both pollen and NPP taxa were included in the analysis in order to detect peatland communities and their relationships with landscape-scale assemblages.

To evaluate temporal changes in palynological richness, rarefaction analysis was applied to the pollen dataset standardised to the minimum pollen count per sample (n = 394) (Birks and Line 1992).

Zonation was determined by visual inspection supported by the main compositional changes identified by the PCAtr. Diagrams and rarefaction calculations were generated with Psimpoll 4.27 (Bennet 2025).

Results

Physicochemical properties and charcoal records

The physicochemical properties and charcoal records are summarised according to the six stratigraphic units identified in the TOX core (Fig. 3).

Unit I (151-140.5 cm; ~11,100-10,350 cal. yr BP) – Organic-rich mineral sediment: This basal unit is characterised by the lowest organic matter (OM) content in the sequence, as reflected by the C, N, and S records. Carbon values range between 9.3% and 18% –

Table 2 Radiocarbon dates in the TOX core from the Toxiza fen (Xistral Mountains, Galicia, Spain)

Laboratory code	Material type	Sample code	Depth (cm)	AMS ^{14}C date BP	cal. yr BP (2σ range)	Probability (%)	Median probability
Beta-649067	Peat	TOX-A-30	29-30	1310 ± 30	1176-1229	49.6	1236
					1234-1236	0.3	
					1242-1293	50.1	
Beta-649068	Peat	TOX-B-60	59-60	2910 ± 30	2961-3159	100	3049
Beta-649069	Peat	TOX-B-90	89-90	3960 ± 30	4295-4333	10.7	4428
					4348-4451	55	
					4464-4520	34.3	
Beta-681301	Peat	TOX-A-105	104-105	5200 ± 30	5906-5999	97.7	5961
					6093-6104	2.3	
Beta-649070	Peat	TOX-A-120	119-120	7880 ± 30	8590-8778	94.3	8675
					8833-8860	3.3	
					8889-8890	0.3	
					8919-8937	1.5	
					8960-8972	0.8	
Beta-649071	organic-rich mineral sediment	TOX-B-151	150-151	9690 ± 30	10876-10941	13.8	11140
					11073-11205	86.1	

Radiocarbon dates are calibrated with the IntCal20 radiocarbon age calibration curve (Reimer et al. 2020) with the software CALIB (Stuiver and Reimer 1993) version 8.20

values typical of organic-rich mineral sediments, but lower than those expected in peat. The C/N ratio increases from 16.2 to 21.8, indicating a transition from moderate to lower OM decomposition. L* values (34.6-42.4) are relatively high, suggesting lighter (less dark) colours. The a* and b* colour coordinates indicate a reddish-yellowish hue, consistent with brownish tone. Both CHAR and microcharcoal influx are low, pointing to limited fire activity during this phase.

Unit II (140.5-123 cm; ~10,350-9075 cal. yr BP) – Brown peat: OM content increases sharply, as shown by higher C, N, and particularly S values – the latter peaking here, likely due to anoxic conditions during peat accumulation due to terrestrialisation. Carbon content ranges from 32.7% to 50.4%, consistent with peat formation. The C/N ratio rises from 24.4 to 27.9, suggesting a low degree of OM decomposition. L* values decrease (29.4-34.7), indicating a slightly darker matrix. Colour coordinates reflect stronger green and yellow hues, contributing to a dark brownish appearance. CHAR shows numerous peaks, whereas microcharcoal influx shows low pronounced changes, suggesting episodic local fire activity with more limited atmospheric input (low regional fire activity). L* values and C content present similar patterns in the peat section of the core (r^2=0.80), as well as L* and C/N ratio (r^2=0.71), pointing to the usefulness of colour parameters as indirect proxies of organic matter content (Sanmartín et al. 2015).

Unit III (123-94 cm; ~9075-4900 cal. yr BP) – Black peat: This unit maintains high and stable OM values. Carbon values range from 43.8% to 52.5%, typical of well-developed peatlands. The C/N ratio (25.6-32.4) continues to suggest a low degree of OM decomposition. L* values (25.5-30.2) are among the lowest, reflecting dark coloration. This unit

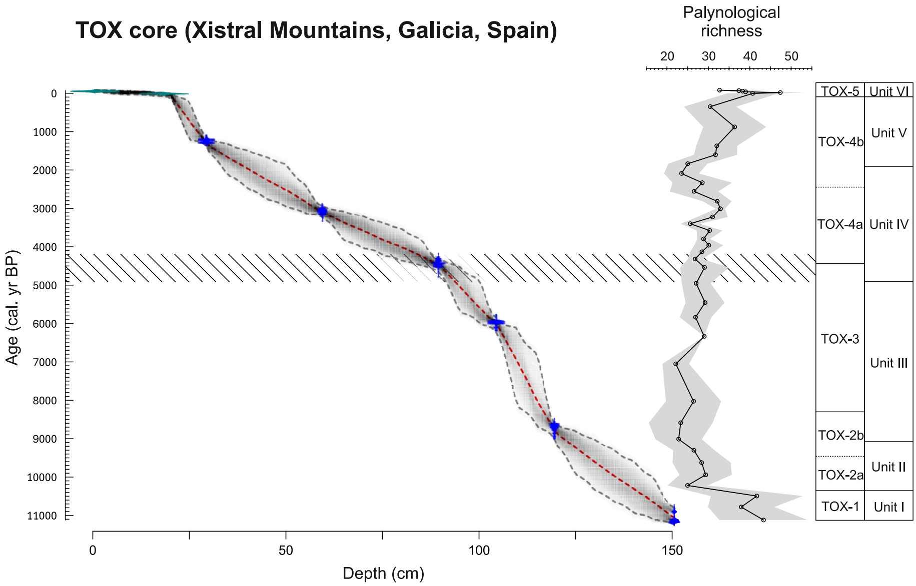

Fig. 2 Age-depth model for the TOX core retrieved from the Toxiza fen (Xistral Mountains, Galicia, Spain). Left: Bayesian age-depth model generated with *Bacon* 2.3 (Blaauw and Christen 2011) integrating six calibrated radiocarbon dates with two independent chronological constrains: the well-documented onset of *Pinus pinaster* afforestation in the Xistral Mountains in 1955 AD (±10 years) at 18.5 cm (Díaz Varela et al. 1997), and the coring year assigned to the uppermost sample (±10 years). Calibrated radiocarbon dates are shown as probability density functions. The grey envelope represents model uncertainty, dashed grey lines indicate the 95% confidence intervals, and the dashed red line marks the best-fit model based on the weighted mean age for each depth. Centre: Palynological richness ($E[T_{394]})$ estimated by rarefaction analysis, with the grey envelope representing the 95% confidence intervals, expressed as the expected number of taxa. Right: Palynological zones and stratigraphic units recognised in the TOX core; the hatched horizontal band marks the sand-rich layer at the base of Unit IV

exhibits the lowest a* and b* values in the entire core, indicating low redness and yellowness colour components, which combine to produce the black hue described stratigraphically. Both CHAR and microcharcoal influx are minimal, suggesting a period of reduced fire activity.

Unit IV (94-40 cm; ~4900-1900 cal. yr BP) – Brown peat with decomposed plant remains: This unit includes a sand-rich layer at its base (94-84 cm; ~4900-4200 cal. yr BP), which disrupted sample milling in some cases. OM remains high, with C values from 40.9% to 52.7%. The C/N ratio reveals two phases: slightly lower values (24.5-29.5) from 94 to 55 cm (~4900-2800 cal. yr BP), and higher values (34.9-39) from 55 to 40 cm (~2800-1900 cal. yr BP), indicating a progression toward very low OM decomposition – consistent with the presence of decomposed plant remains. L* values are slightly higher than in the previous unit (27.4-31.0), indicating a lighter brownish tone. The a* and b* values increase, reflecting enhanced redness and yellowness. CHAR and microcharcoal influx are low within the sand-rich layer, increase sharply above it (up to 65 cm, ~3300 cal. yr BP), decrease (up to 2440 cal. yr BP), and increase again toward the top, suggesting varying fire regimes.

Unit V (40–20.5 cm; ~1900-85 cal. yr BP) – Stratified brown-black peat with charcoal fragments: Here, OM remains high, though C content decreases from 50.5% to 40.3%, while N and S levels rise. This results in a decreasing C/N ratio (33.2 to 21), suggesting a

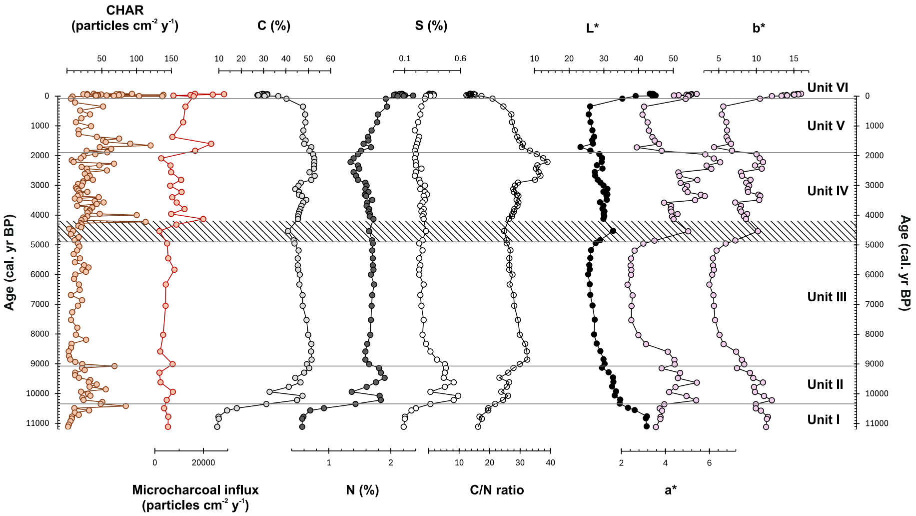

Fig. 3 Charcoal and physicochemical records of the TOX core retrieved from the Toxiza fen (Xistral Mountains, Galicia, Spain) plotted against age. Left: Macrocharcoal accumulation rate (CHAR) and microcharcoal influx records. Centre: CHNS elemental analysis records. Right: Colorimetry records. The detected stratigraphic units are also included, and the hatched horizontal band marks the sand-rich layer at the base of Unit IV. Charcoal and physicochemical records plotted against depth are in Supplementary Fig. 1

shift from very low to low OM decomposition. L* values (23.3-35.3) indicate a dark matrix. The a* and b* values are low, reflecting lower redness and yellowness components – consistent with a dark hue. This unit records high CHAR and microcharcoal influx at the bottom of the unit, highlighting intense fire activity up to 1300 cal. yr BP at both local and regional scales.

Unit VI (20.5–0 cm; < ~85 cal. yr BP) – Brown peat with mineral input and surface vegetation: This uppermost unit shows reduced OM content compared to previous peat layers. Carbon values range from 36.6% to 27.3%, the lowest in the peat section – most likely reflecting the transition between de acrotelm and catotelm –, while N and S levels increase. The low C/N ratio (12.4-17.3) suggests more advanced decomposition. L* values are the highest in the core (39.2-44.9), indicating lighter colours. The a* and b* values reach maximum values as well, reflecting increased redness and yellowness – resulting in a light brown appearance. Both CHAR and microcharcoal influxes peak at onset of the unit and remain high, indicating continued recent fire influence.

Palynological results: zonation and PCAtr

Palynological preservation and diversity were excellent, yielding 121 pollen types and 61 NPP types (Fig. 4 in age, Supplementary Fig. 2 in depth). Vegetation surveys show that several taxa currently present in the fen are represented in the palynological diagram only at a broader taxonomic resolution (e.g. Cyperaceae undiff., Poaceae undiff., Ericaceae undiff.), whereas others are palynologically absent despite being locally present (Table 1). This reflects both the limited taxonomic resolution of some pollen types and differences in pollen production and dispersal, as many of the undetected taxa are entomophilous or self-

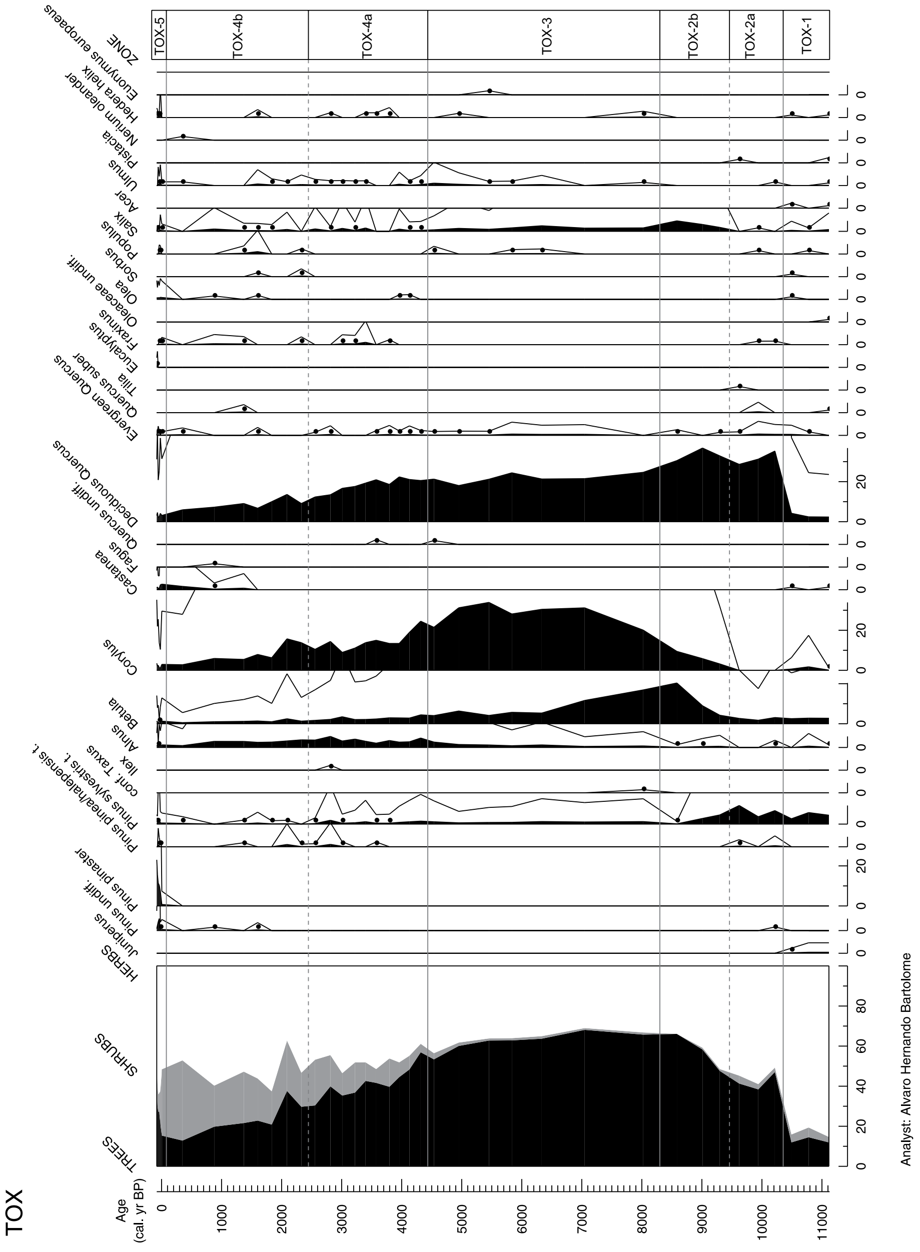

Fig. 4 Palynological percentage diagram of the TOX core retrieved from the Toxiza fen (Xistral Mountains, Galicia, Spain) plotted against age. The filled silhouettes show the percentage curves of the taxa, while the white silhouettes show the ×10 exaggeration curves. Dots stand for percentages below 0.5%. The detected palynological zones are also included. The palynological diagram plotted against depth is in Supplementary Fig. 2

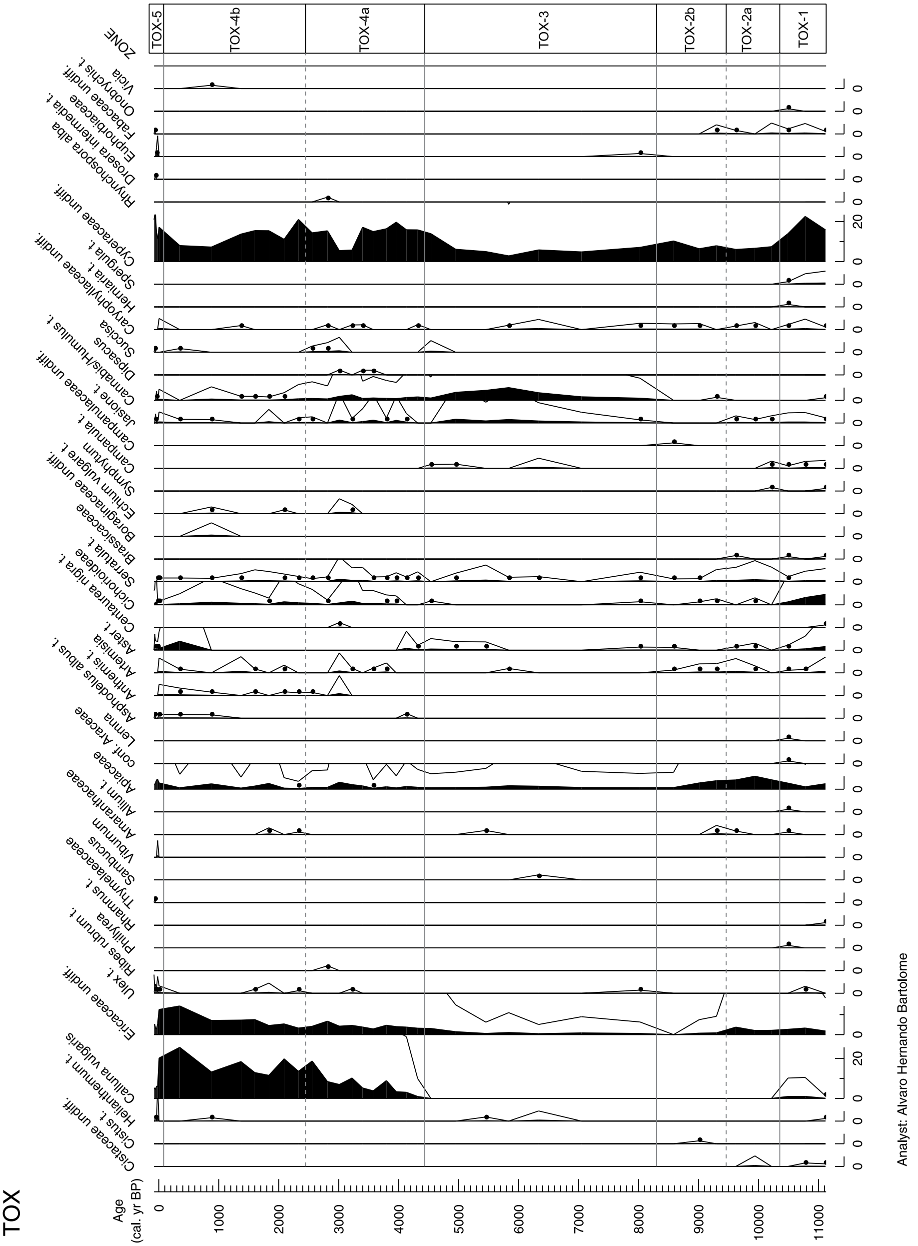

Figure 4 (continued)

pollinated. The only undetected anemophilous group is Juncaceae, despite its occurrence in the modern vegetation (Table 1), probably because its thin, weakly sporopolleninised exine makes it especially susceptible to corrosion and mechanical loss during burial and laboratory processing (Faegri et al. 1989).

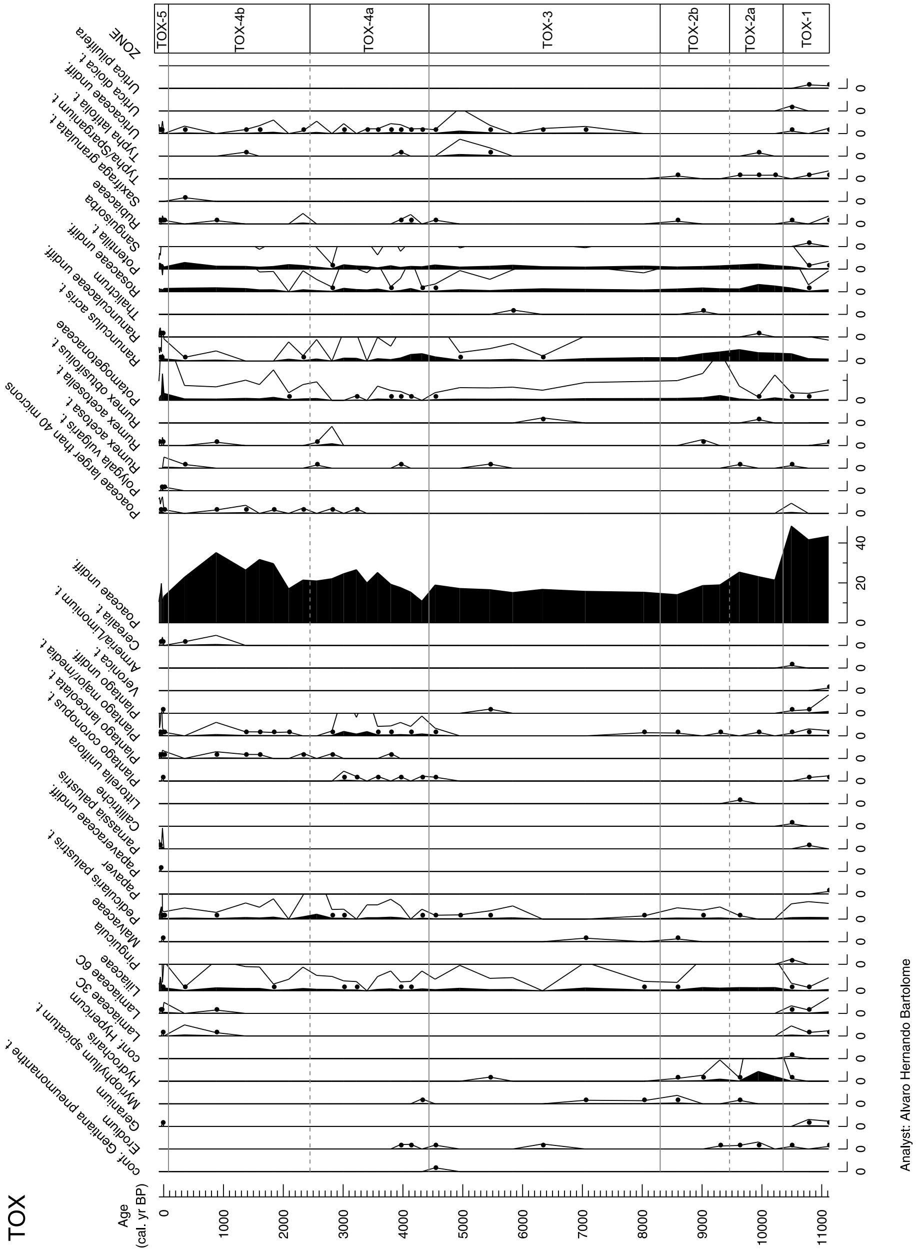

Figure 4 (continued)

The main palynological changes identified are summarised across five palynological zones, described in Table 3, that broadly align with the three Holocene stages/ages (Walker et al. 2019): Greenlandian (zone TOX-1: ~11,100-10,350 cal. yr BP, and zone TOX-2: ~10,350-8300 cal. yr BP), Northgrippian (zone TOX-3: ~8300-4430 cal. yr BP), and

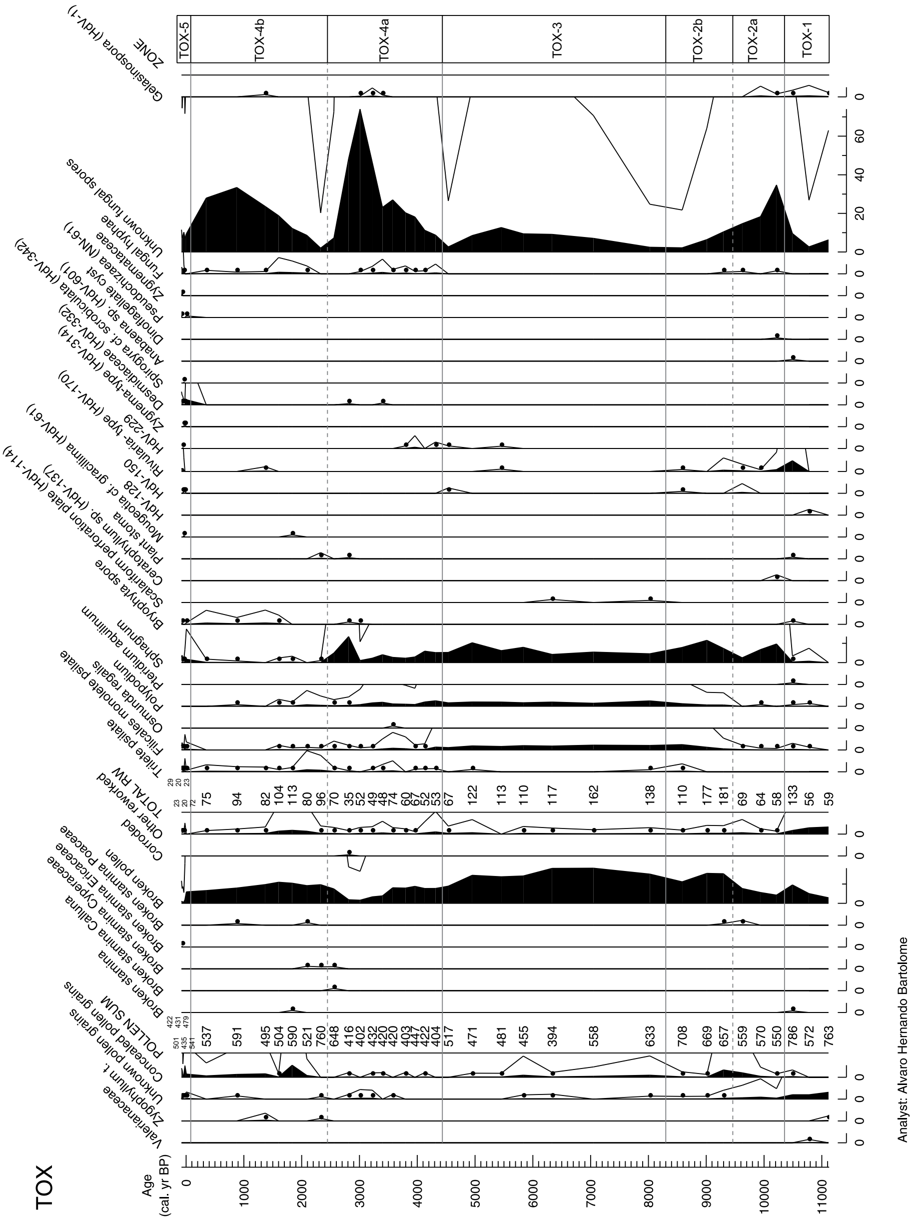

Figure 4 (continued)

Meghalayan (zone TOX-4: ~4430-85 cal. yr BP, and zone TOX-5: ~85-present). Rarefaction analysis standardised to the minimum pollen count (n = 394) indicates higher pollen richness in the basal and upper sections of the sequence, corresponding to the Greenlandian and Meghalayan stages, whereas values remain comparatively stable during the middle part of the record associated with the Northgrippian stage (Fig. 2). In addition, the PCAtr yielded

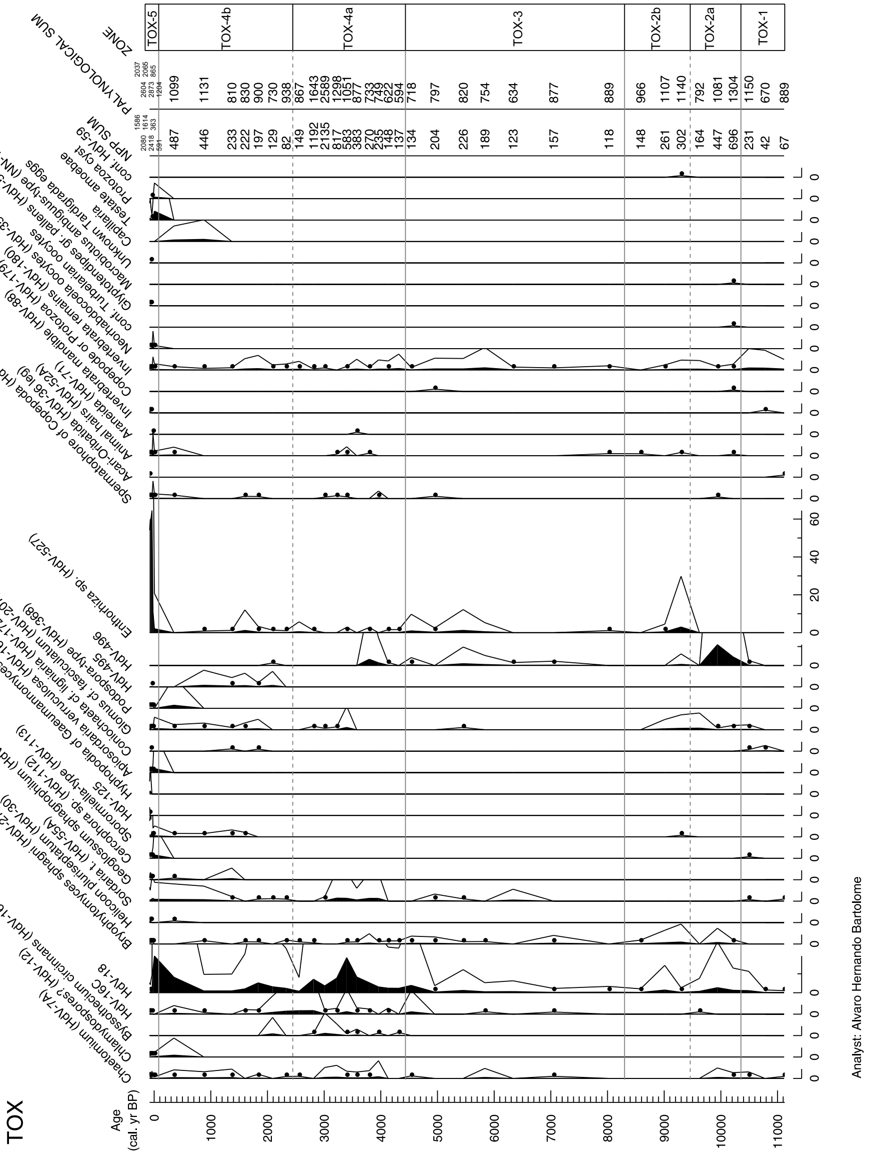

Figure 4 (continued)

five principal components explaining 93.5% of the total palynological variance. Fig. 5 displays the factor scores of selected taxa, and the fractionation of communalities (i.e., squared factor loadings) explained per sample plotted against age (Supplementary Fig. 3 in depth; Supplementary Table 1 for factor scores of all taxa).

The **first principal component (PC1)** explains 32.3% of the total variance. It is strongly influenced by high positive scores of *Corylus* and deciduous *Quercus*, with moderate positive contributions from *Betula*, *Sphagnum*, Cyperaceae undiff. and Poaceae undiff. In con-

Table 3 Description of the five palynological assemblage zones of the TOX core from the Toxiza fen (Xistral Mountains, Spain)

Zone		Characteristics
TOX-1 (151-140.5 cm; ~11,100-10,350 cal. yr BP)		**TREES**: Tree pollen is lowest in the record (~10-15%), composed of low values of *Pinus sylvestris* t., *Betula*, deciduous *Quercus*, and *Corylus*. *Juniperus* occurs only in this zone. **SHRUBS**: Shrub pollen is scarce (~5%), with occasional Ericaceae undiff. and *Calluna vulgaris*. **HERBS**: Herbs dominate the assemblage (~80-85%), commanded by Poaceae undiff. and Cyperaceae undiff., with minor Cichorioideae and Apiaceae. **NPP**: Generally sparse, a peak of *Rivularia*-t. (HdV-170) occurs at the top of the zone.
TOX-2 (140.5-116.5 cm; ~10,350-8300 cal. yr BP)	**TOX-2a** (140.5-128.5 cm; ~10,350-9460 cal. yr BP)	**TREES**: Increase to ~40-50%, dominated by deciduous *Quercus*; *Pinus sylvestris* t. and *Betula* remain low; *Corylus* is absent. **SHRUBS**: Remain scarce (<5%), exclusively by Ericaceae undiff. **HERBS**: Still dominant (~50-60%) but reduced compared to TOX-1; Poaceae undiff., Cyperaceae undiff., and Cichorioideae decrease, while Apiaceae increases. Hydro-hygrophilous taxa (*Hydrocharis* and *Ranunculus acris* t.) increase. **NPP**: Fungal spores undiff. are high *Sphagnum*, HdV-496, HdV-18, and *Bryophytomyces sphagni* (HdV-27) increase. *Rivularia*-t. (HdV-170) persists. *Glomus* cf. *fasciculatum* (HdV-270) shows a continuous curve. Fungal hyphae are present.
	TOX-2b (128.5-116.5 cm; ~9460-8300 cal. yr BP)	**TREES**: Continue to increase (~50-60%), still dominated by deciduous *Quercus*. *Pinus sylvestris* t. decreases; *Betula* and *Salix* increase initially, followed by *Corylus*. **SHRUBS**: Nearly absent. **HERBS**: Decrease to ~40%, mainly due to lower Poaceae undiff. and Apiaceae. **NPP**: Fungal spores undiff., *Rivularia*-type (HdV-170), and HdV-496 decrease. *Sphagnum* remains persistent with *Bryophytomyces sphagni* (HdV-27). *Polypodium* and Filicales monolete psilate increase. *Enthorhiza* sp. (HdV-527) shows a distinct peak.
TOX-3 (116.5-88.5 cm; ~8300-4430 cal. yr BP)		**TREES**: High and stable (~60-65%), the maximum of the profile; assemblage dominated by deciduous *Quercus* (lower values than before) with marked increase in *Corylus* and decrease in *Betula* and *Salix*; *Ulmus*, *Populus* and *Alnus* are continuously present. **SHRUBS**: Nearly absent. **HERBS**: ~40-50%; hydro-hygrophytes (Apiaceae, *Hydrocharis*, and *Ranunculus acris* t.) decline. In contrast, *Cannabis/Humulus* t. and *Jasione* t. increase; Urticaceae undiff. becomes continuous ~7000 cal. yr BP. **NPP**: Fungal spores undiff., *Rivularia*-type (HdV-170), HdV-496, HdV-18, and *Glomus* cf. *fasciculatum* (HdV-270) remain low. *Sphagnum* is consistently present and notable, together with *Bryophytomyces sphagni* (HdV-27). *Polypodium* and Filicales monolete psilate reach their highest values. *Enthorhiza* sp. (HdV-527) appears at the top of the zone.

Table 3 (continued)

Zone		Characteristics
TOX-4 (88.5-20.5 cm; ~4430-180 cal. yr BP)	**TOX-4a** (88.5-48.5 cm; ~4430-2440 cal. yr BP)	**TREES**: Decrease from ~50% to ~30%, mainly *Corylus* and deciduous *Quercus*; *Betula*, *Salix*, and *Ulmus* also decrease; *Populus* disappears. *Alnus* and *Fraxinus* become better represented. **SHRUBS**: Increase from near absent to ~20%, with *Calluna vulgaris* dominant, followed by Ericaceae undiff. **HERBS**: Slightly increase (~50 to ~55%), mainly Cyperaceae undiff. and, to a lesser extent, Poaceae undiff. Other herbs increasing include Cichorioideae, *Pedicularis palustris* t., *Plantago major/media* t., and *Plantago coronopus* t. *Cannabis/Humulus* t., *Jasione* t., and Potamogetonaceae decrease. **NPP**: *Sphagnum* shows and overall decrease but peaks near the top. Fungal spores undiff. and HdV-18 rise before declining. Filicales monolete psilate and *Polypodium* decrease, while Trilete psilate increases. Also present: *Chaetomium* (HdV-7A), *Byssothecium circinans* (HdV-16A), HdV-16C, and *Sordaria* t. (HdV-55A). Fungal hyphae occur in the first half, *Glomus* cf. *fasciculatum* (HdV-270) in the second.
	TOX-4b (48.5-20.5 cm; ~2440-85 cal. yr BP)	**TREES**: Continue the decrease to ~10%, due to ongoing declines in *Corylus* and deciduous *Quercus*, along with *Betula* and *Alnus*. **SHRUBS**: Increase to ~30%, with *Calluna vulgaris* dominant, followed by Ericaceae undiff. *Ulex* t. present. **HERBS**: Slight overall increase, mainly Poaceae undiff., Cichorioideae, and Potamogetonaceae. Cyperaceae undiff., *Ranunculus acris* t., *Plantago major/media* t., *Cannabis/Humulus* t., and *Jasione* t. decrease. **NPP**: *Sphagnum* declines to near zero. Filicales monolete psilate and *Polypodium* decrease. Fungal spores undiff. are low in the first half and increase thereafter, mirroring Fungal hyphae. HdV-18, *Chaetomium* (HdV-7A), *Byssothecium circinans* (HdV-16A), HdV-16C, and *Sordaria* t. (HdV-55A) show lower values. HdV-496 appears for the first time and becomes continuous.
TOX-5 (20.5-0 cm; ~85 cal. yr BP-present)		**TREES**: Increase from ~10% to ~40%, driven by *Pinus pinaster*, *Pinus* undiff., *Castanea*, and *Olea*; *Eucalyptus* appears in the uppermost samples. Temperate trees values continue an overall decline. **SHRUBS**: Decrease to ~10%, mainly due to declines in *Calluna vulgaris* and Ericaceae undiff.; *Ulex* t. and *Helianthemum* t. increase. **HERBS**: Slight overall increase, due to Cyperaceae undiff., Apiaceae, *Aster* t., Liliaceae, *Pedicularis palustris* t., *Parnassia palustris*, *Plantago major/media* t., *Cerealia* t., Potamogetonaceae, and *Ranunculus acris* t. Poaceae undiff. decreases markedly, as do *Cannabis/Humulus* t. and *Jasione* t. **NPP**: Assemblage dominated by high *Enthorhiza* sp. (HdV-527). Also increasing are *Sordaria* t. (HdV-55A), *Cercophora* sp. (HdV-112), *Sporormiella*-t. (HdV-113), *Apiosordaria verruculosa* (HdV-169), *Podospora*-t. (HdV-368), Spermatophores of Copepoda (HdV-28), Testate amoebae, Animal hairs (HdV-52A), Chlamydospores? (HdV-12), Desmidiaceae (HdV-332), *Rivularia*-t. (HdV-170), and Filicales monolete psilate. Fungal spores undiff. and *Sphagnum* are low, although *Sphagnum* shows a small peak at the zone base.

trast, Fungal spores undiff. and *Enthorhiza* sp. (HdV-527) show moderate negative scores. PC1 assemblage likely reflects the significance of temperate deciduous woodlands at landscape scale, and, at the local scale, the presence of a *Sphagnum*-rich peatland with sedges and grasses. PC1 explains most of the variance in samples from zone TOX-3, and a substantial proportion in samples from zone TOX-2b and the bottom part of zones TOX-4a and TOX-4b (Fig. 5).

The **second principal component (PC2)** accounts for 22.9% of the total variance. Large positive scores are observed for Fungal spores undiff. and *Calluna vulgaris*, while HdV-18, Ericaceae undiff., and Poaceae undiff. show moderate positive scores. Negative scores are recorded for *Betula* and *Enthorhiza* sp. (HdV-527). PC2 assemblage likely captures an Ericaceae-rich peatland with Poaceae. Ericaceae undiff. likely represents local *Erica mackaiana* stands, whereas *Calluna vulgaris* may reflect both, local stands as well as the land-

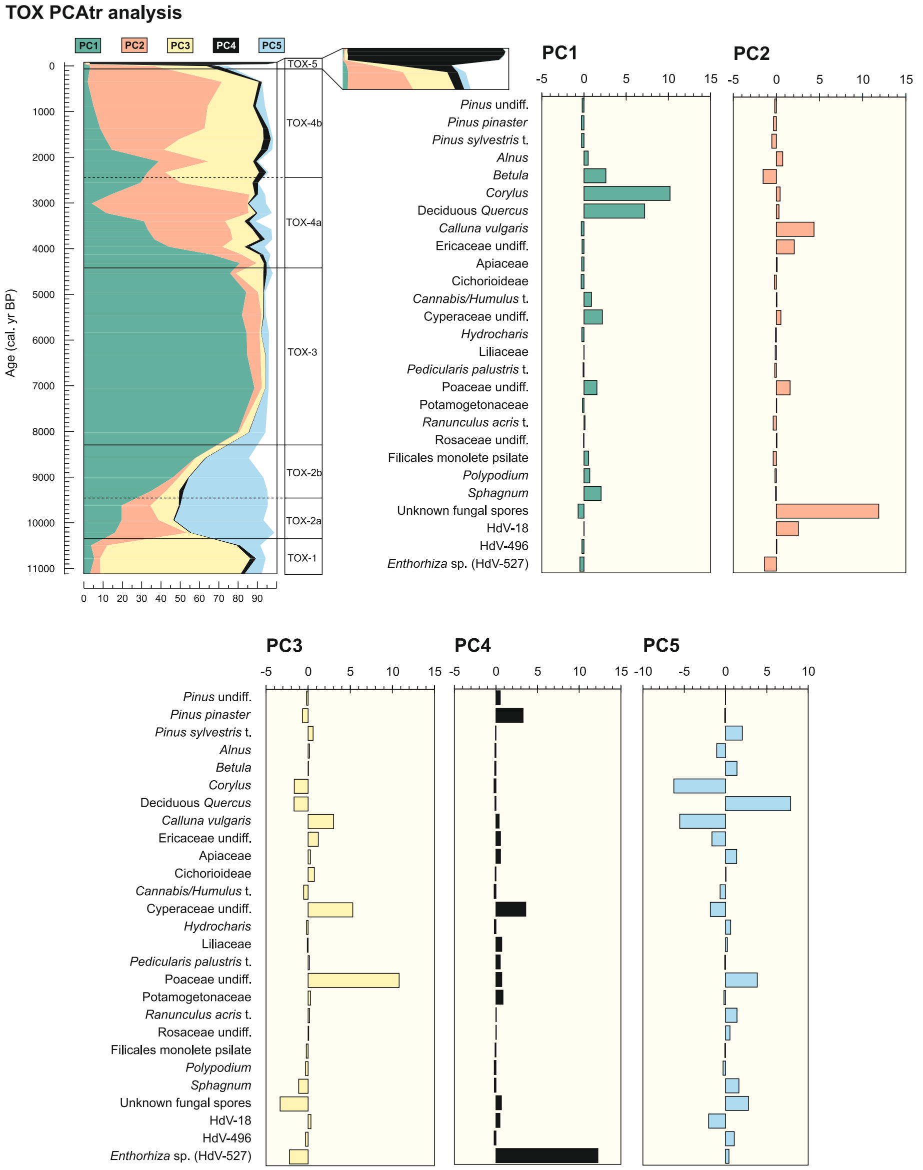

Fig. 5 Principal component analysis results (transposed matrix) of the palynological dataset of the TOX core retrieved from the Toxiza fen (Xistral Mountains, Galicia, Spain). Top left: Age records of the partial communalities (squared factor loadings) of the five principal components explaining the variation of the palynological signal (depth records of the partial communalities (i.e., squared factor loadings) are in Supplementary Fig. 3). The detected palynological zones are also included. Top right and bottom: Factor scores of the five principal components obtained (selected taxa, the factor scores for all taxa are in Supplementary Table 1

scape-scale heathland vegetation, the latter suggested by the negative score of *Betula*. The strong positive score of Fungal spores undiff. may suggest increased soil disturbance, while the positive score of HdV-18 could reflect changes in fen hydrology (Silva-Sánchez et al. 2014). The negative score of *Enthorhiza* sp. (HdV-527) – a fungal NPP associated with root systems in disturbed, clay-rich soils (van Geel et al. 1983) – suggests absence of rapid clay sedimentation. The contribution of PC2 to the total variance is noteworthy in samples from zones TOX-4a and TOX-4b, and also important in samples from zone TOX-2a (Fig. 5).

The **third principal component (PC3)** explains 17.3% of the total variance. It is characterised by large positive scores for Poaceae undiff., Cyperaceae undiff., and *Calluna vulgaris*, while Ericaceae undiff. and Cichorioideae present moderate positive scores. Conversely, large negative scores are recorded for Fungal spores undiff., *Enthorhiza* sp. (HdV-527), *Corylus*, and deciduous *Quercus*, while *Sphagnum* shows a moderate negative score. PC3 assemblage likely reflects wet meadows with heathland rather than a peatland proper. Furthermore, Cichorioideae could be pointing to an open landscape, as well the negative scores of *Corylus* and deciduous *Quercus*. PC3 accounts for most of the variance in samples from zone TOX-1 and a significant fraction in samples from zone TOX-4b (Fig. 5).

The **fourth principal component (PC4)** contributes 12.1% to the total variance and is characterised by large positive scores of *Enthorhiza* sp. (HdV-527), Cyperaceae undiff., and *Pinus pinaster*, along with moderate positive scores of Potamogetonaceae, Poaceae undiff., Liliaceae, Fungal spores undiff., Apiaceae, Ericaceae undiff., *Pinus* undiff., and *Pedicularis palustris* t. PC4 assemblage likely reflects a local Cyperaceae-rich peatland with the presence of hydro-hygrophilous taxa (e.g., Potamogetonaceae, *Pedicularis palustris* t.), coexisting with an afforested landscape dominated by *Pinus pinaster*. The very large positive score of *Enthorhiza* sp. (HdV-527) points to clay-rich sediment input (van Geel et al. 1983) likely linked to erosion from afforestation. PC4 explains most of the variance in samples from zone TOX-5 (Fig. 5).

The **fifth principal component (PC5)** explains 8.9% of the total variance. PC5 is characterised by large positive scores of deciduous *Quercus* and Poaceae undiff., with moderate positive scores of Fungal spores undiff., *Pinus sylvestris* t., *Sphagnum*, *Betula*, *Ranunculus acris* t., Apiaceae, HdV-496, and *Hydrocharis*. In contrast, *Corylus* and *Calluna vulgaris* have large negative scores, while HdV-18, Cyperaceae undiff., Ericaceae undiff., and *Alnus* show moderate negative scores. PC5 assemblage likely reflects the importance of regional oak woodlands, along with *Pinus sylvestris* t. and *Betula* formations, in the absence of *Corylus*. At the local scale, it reflects a Poaceae-rich vegetation with a hydro-hygrophilous assemblage composed of *Sphagnum*, *Ranunculus acris* t., Apiaceae, and *Hydrocharis*. The presence of HdV-496 – a NPP associated with graminoid-rich peat (van Smeerdijk 1989) – supports the role of Poaceae in the local assemblage. PC5 explains an important fraction of the variance in samples from zones TOX-2a and TOX-2b (Fig. 5).

Discussion

In this section, we integrate the multi-proxy evidence to develop a palaeoenvironmental, chronological, and botanical interpretation of the fen record.

Greenlandian: mire formation and transition from Poaceae-rich to *Sphagnum*-rich fen under climate forcing (TOX-1 and TOX-2: ~11,100-8300 cal. yr BP)

The development of Galician mires has been framed in three different phases (Pontevedra-Pombal et al. 2006): (i) an early Holocene phase during which fens established (~11,000-8500 cal. yr BP), (ii) a mid-Holocene interval (~7800-7100 cal. yr BP) that saw the inception of both fens and bogs, and (iii) a late to mid-Holocene phase (~6000-2000 cal. yr BP) characterised by bog expansion and fen stabilisation. Within this scheme, the Toxiza (TOX) fen falls in the first phase.

The basal organic-rich mineral sediments at TOX core are dated at ~11,100 cal. yr BP. Peat accumulation started at ~10,350 cal. year BP, when Unit I (organic-rich mineral sediment) gives way to the brown peat of Unit II (Fig. 1). This lithological shift coincides with rises in OM proxies (i.e., C, N, S) and changes in colour parameters (Fig. 3). Carbon contents of 32.7-50.4% are consistent with peat, and the small valley setting of TOX (Fig. 1) implies a strong minerogenic/minerotrophic influence on peat formation. Palynological data supports physicochemical proxies and indicate a coherent ecological transition: from wet meadow communities (zone TOX-1; captured by PC3) to a transitional fen with an importance of Poaceae in the local vegetation, consistent with the presence of HdV-496, a NPP indicative of graminoid-rich peat (van Smeerdijk 1989), accompanied by *Sphagnum* and hydro-hygrophilous assemblage (*Ranunculus acris* t., Apiaceae, and *Hydrocharis*), represented by PC5 from zone TOX-2a (Fig. 5). We infer a terrestrialisation trajectory between ~10,350 and ~8300 cal. year BP, during which elevated PC5 scores account for a substantial fraction of the samples' variance (zones TOX-2a and TOX-2b). A rising water table likely created small ponds in the valley where floating mats of *Sphagnum* and other hydro-hygrophilous taxa, such as the floating macrophytes (*Hydrocharis*, *Ranunculus* subgen. *Batrachium*) developed. This aquatic vegetation trapped plant detritus, progressively infilling open water with peat. During the first phase of terrestrialisation (zone TOX-2a), the forming peat seems to be an Ericaceae-rich fen, as pointed by PC2 scores, that gradually shifted towards a *Sphagnum*-rich fen (zone TOX-2b), concurrently with an increase in PC1 scores explaining the variance of the samples. Locally, the PC3→PC5(PC2)→PC1 sequence thus tracks fen initiation and consolidation, considering zone TOX-2 as a transitional phase in which terrestrialisation took place (Fig. 6). This is further supported by several key fen taxa recorded in the modern mire that are represented in the Holocene record only through broader pollen categories (Table 1), particularly Cyperaceae and Poaceae, which remain informative for reconstructing local mire development and terrestrialisation processes. At the landscape scale, peat inception at TOX broadly aligns with a transition from open landscape (zone TOX-1; captured by PC3) to initial oak woodland expansion (captured by PC5). Moreover, it somewhat aligns with the importance of heathland (captured by PC2) in zone TOX-2a, culminating in more extensive deciduous woodlands dominated by deciduous *Quercus*, *Corylus*, and *Betula* (gradual replacement of PC5 by PC1 in zone TOX-2b; Fig. 6).

Comparable timing of peat inception is reported elsewhere in the Xistral Mountains. At CVM – now an intact raised bog – coring indicates fen conditions at ≥10,000 cal. yr BP (basal sediment not reached) followed by rapid transition to a raised bog at ~9500 cal. yr BP (Pontevedra-Pombal et al. 2019). At TPD, another raised bog not far away from TOX, basal sediments dates to ~10,500 cal. yr BP, fen conditions begin at ~10,300 cal. yr BP, persist until ~8200 cal. yr BP, and then grade into bog, stabilising at ~6700 cal. yr BP (Mar-

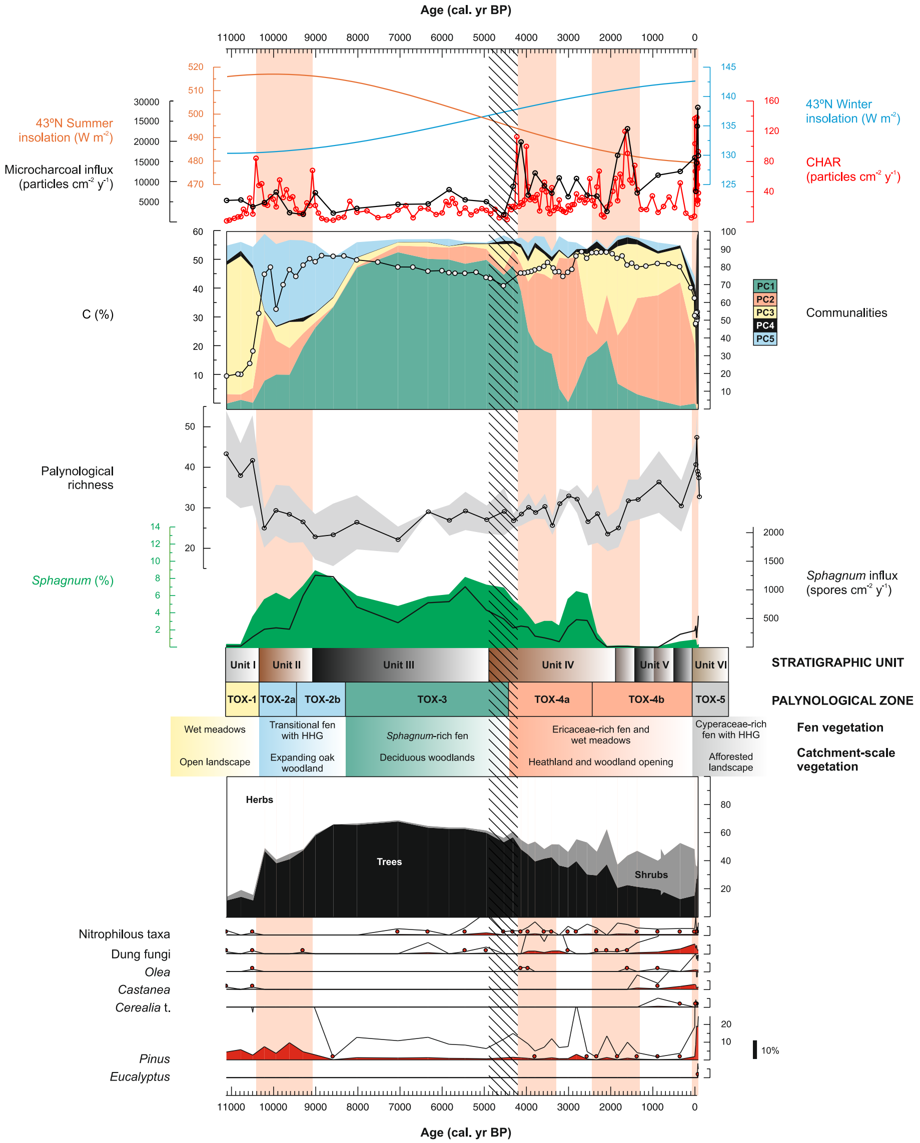

Fig. 6 Summary of Holocene environmental change recorded in the TOX core from the Toxiza fen (Xistral Mountains, Galicia, Spain). From top to bottom: summer and winter insolation at 43º N (Laskar et al. 2004); fire activity inferred from charcoal, with microcharcoal influx representing particles <150 µm and CHAR particles >150 µm; carbon content (%C) and partial communalities (i.e., squared factor loadings) of the five principal components derived from the PCA on the transposed palynological matrix (PCAtr); palynological richness ($E[T_{394}]$) estimated by rarefaction analysis; *Sphagnum* percentage and influx (three-sample moving averages);stratigraphic units and palynological zones; synthesis of reconstructed fen-scale and catchment-scale vegetation; percentages of trees, shrubs and herbs; nitrophilous taxa (sum of *Plantago lanceolata* t. and Urticaceae undiff.); dung fungi (sum of *Sordaria* t., *Sporormiella* t., *Cercophora* sp., *Apiosordaria*, and *Podospora* t.); and selected anthropogenic and afforestation indicators: *Olea*, *Castanea*, *Cerealia* t., *Pinus* (sum of *Pinus* undiff., *Pinus pinaster*, *Pinus pinea/halepensis* t., and *Pinus sylvestris* t.) and *Eucalyptus*. For the palynological curves, filled silhouettes show the taxa percentage values and white overlays show ×10 exaggeration. Dots mark values < 0.5%. Red bands highlight pyrogenic phases, and the hatched band marks the sand-rich layer at the base of Unit IV. HHG = hydro-hygrophilous plants

tínez Cortizas et al. 2020). Other studies of current bogs indicate no reference to peatland structure, but peat is described as the material under study. For instance, the continuous peat accumulation spanning over the last ~10,000 years and ~8500 years in the Chan do Lamoso bog (CDL) and the central sector of the Pena da Cadela bog (PDC2) respectively (Ramil-Rego et al. 1998; Muñoz Sobrino et al. 2005; Mighall et al. 2023); or and the transition from sediment to peat is dated back to ~10,900 cal. yr BP at PVE (Ramil-Rego et al. 1998). Collectively, the timing of this first phase of peat inception at the Xistral Mountains, and subsequent trajectories, appears linked to climate forcing, particularly orbital/solar forcing (Fig. 6).

Astronomical solutions (Laskar et al. 2004) show that at 43° N the Early Holocene featured high summer insolation (peaking at ~10,000 cal. yr BP) and minimum winter insolation, i.e., strong seasonality with warm summers and long, cold winters. This configuration favoured woodland expansion from the start of the Holocene – from the Late Glacial pine and birch remnants to deciduous *Quercus* – culminating in more extensive deciduous woodlands dominated by deciduous *Quercus*, *Corylus*, and *Betula*. Pollen-based climate reconstructions of Iberia indicate cold, dry winters during this interval (Liu et al. 2023), the TOX pollen record shows the importance of *Artemisia* and Cichorioideae (Fig. 4), and geochemical records from TPD detect phases of dust deposition during the early Holocene in the Xistral, suggesting also dry summers (Martínez Cortizas et al. 2020). However, enhanced summer insolation also increased evapotranspiration, reducing soil moisture and elevating wildfire risk. In the TOX core, CHAR and, to a lesser extent, microcharcoal influx, during Unit II (~10,350-9075 cal. yr BP) attest to episodic fire activity. PC2 also becomes important in zone TOX-2a, coeval with this phase of increased fire activity, and indicates the spread of heathland likely related to the fires (Fig. 6). Such disturbances likely altered catchment hydrology, promoting runoff and facilitating fen establishment by terrestrialisation (i.e., TOX, CVM, TPD).

By ~8300 cal. yr BP, TOX records a *Sphagnum*-rich fen, while at landscape scale deciduous woodlands dominated by deciduous *Quercus* and *Corylus* prevailed – marking the close of the Early Holocene. Macroremains evidence for this interval is scarce, and hydro-hygrophytes are not discussed in detail in the limited early Holocene pollen datasets. Nevertheless, the CVM macroremain records show the shift from a monocots-rich fen to an Ericaceae-rich bog at ~9500 cal. yr BP (Castro 2017). In addition, the Pena Vella bog (PVE) pollen record places woodland expansion at ~10,900 cal. yr BP, and the CDL and PDC2 records – whose basal ages are ~10,000 and ~8500 cal. yr BP, respectively – show extensive deciduous woodlands by their starts (Ramil-Rego et al. 1998; Muñoz Sobrino et al. 2005; Mighall et al. 2023). The latter two, analysed at higher resolution than TOX, resolve the 8.2 cal. ka BP event as short-lived forest retreats, whereas PVE appears to contain a peat hiatus covering that event.

Northgrippian hydrological mire stability: *sphagnum*-rich fen during the Holocene climatic optimum (TOX-3: ~8300-4430 cal. yr BP)

Astronomical solutions indicate progressive decline in summer insolation and a rise in winter insolation at 43° N through the mid-Holocene, weakening seasonality and improving effective moisture relative to the early Holocene. Therefore, by mid-Holocene summers have become less extreme and winters somewhat milder – the climate becomes more oceanic, i.e., temperate and humid. The chronological interval from ~8000 to ~5000 cal. yr BP is widely recognised as the Hypsithermal or Holocene climate optimum (HCO) – the warmest and wettest chronozone in much of Europe. In Galicia, temperatures at the HCO peak were ~2-3 ºC above present, with higher humidity (Martínez Cortizas et al. 2009). Therefore, a more favourable balance between precipitation and evapotranspiration prompted the consolidation of early Holocene peatlands and the initiation of new mires (Pontevedra-Pombal et al. 2006), including PVO by ~8000 cal. yr BP (Kylander et al. 2005), Chan da Cruz (CDC) by ~6700 cal. yr BP (Ramil Rego and Aira Rodríguez 1993b), Pena Veira (PVI) by ~6290 cal. yr BP (Ramil Rego and Aira Rodríguez 1993a), and BLL (=BCG) by ~5400 cal. yr BP (Martínez Cortizas et al. 2005; Mighall et al. 2006).

In this context, the TOX record shows a fully established, *Sphagnum*-rich fen by ~8000 cal. yr BP, remaining stable for almost four millennia as indicated by PC1 explaining nearly all variance in zone TOX-3. The role of *Sphagnum* during both the terrestrialisation phase and the mid-Holocene is supported not only by spore percentages, that sometimes could be an artefact as spores are excluded from the pollen sum, but also by spore influx, which mirrors the same trends throughout the profile (Fig. 6). Consistently high and stable organic-matter proxies (C, N, S) and dark peat colour further indicate sustained waterlogging, while mineral dust inputs at nearby TPD were subdued (Martínez Cortizas et al. 2020). In line with the Bayesian age–depth model, accumulation rates remained comparatively low during the mid-Holocene (Fig. 2), consistent with autogenic consolidation and steady – but not rapid – peat accretion under persistently wet conditions. Both CHAR and microcharcoal influx are lower than in the early Holocene, pointing to reduced fire activity under cooler summers and higher moisture availability (Fig. 6).

Organic-molecular markers from modern plants and the ~8000-year-old PVO profile reconstruct a fen-to-bog trajectory, with transition at ~6500-6200 years ago (Schellekens et al. 2011). In the fen interval, intense organic matter decomposition hampered clear taxon-to-biomarker correlations, limiting the ability to assign species contributions to peat composition. By contrast, the bog interval shows a signature dominated by *Carex durieui*, *Agrostis curtisii*, *Festuca rubra*, *Molinia caerulea*, with intermittent *Eriophorum angustifolium* and minor inputs from other Cyperaceae, Poaceae and *Sphagnum* spp. This relatively stable bog assemblage likely reflects HCO climate stability. Notably, whereas TOX remained a *Sphagnum*-rich fen, PVO was monocots-dominated, a difference plausibly arising from hydrology: as a bog, PVO would have been drier as it is not connected to catchment waters due to its location in a mountaintop and, therefore, absence of catchment, while TOX retained minerotrophic inputs under humid HCO conditions. Macroremain data from CVM similarly suggest that HCO bog vegetation tolerated drier settings than fen vegetation, with stronger representation of monocots and Ericaceae (notably *Erica mackaiana*; Castro 2017).

Climatic and hydrological stability during the HCO favoured not only mire systems but also temperate woodlands. TOX pollen indicates maximum deciduous woodland cover (deciduous *Quercus*, *Corylus*, and *Betula*) in zone TOX-3 (captured by PC1; Fig. 6). Mid-Holocene mesophilous woodland dominance is echoed across Xistral pollen records: CDL, PDC2, CDC, PVI, and BLL (BCG) (Ramil Rego and Aira Rodríguez 1993a, b; Ramil-Rego et al. 1998; Martínez Cortizas et al. 2005; Muñoz Sobrino et al. 2005; Mighall et al. 2006, 2023). In addition, other pollen and/or pedoanthracological results of Galician mires, lakes and colluvial soils support the HCO woodland apogee (Ramil-Rego et al. 1998; Muñoz Sobrino et al. 1997, 2005; Santos et al. 2000; Kaal et al. 2011; López-Merino et al. 2012).

Extensive woodland would have enhanced soil-moisture retention and limited soil erosion by reducing runoff. Overall, productivity at both mire and landscape scales likely peaked during the mid-Holocene. The HCO thus represents a phase of hydrologically stable, carbon-accreting fens and expanding bogs across the Xistral, governed primarily by orbital forcing and minimally modified by disturbance.

Meghalayan mire disturbance: intensified human impact and the shift to an Ericaceae-rich fen (TOX-4: ~4430-85 cal. yr BP)

Continued orbital evolution at 43° N during the late Holocene reduced summer insolation and increased winter insolation, further moderating seasonality (Laskar et al. 2004). Superimposed on this orbital trend, pronounced centennial–millennial oscillations occurred – including the 4.2 ka event, Iron Age cooling (~2.8 ka), Roman Warm Period, Medieval Climate Anomaly, Dark Ages Col Period, and Little Ice Age – which modulated effective moisture and temperature; many of which are recorded in Galician archives (Martínez Cortizas et al. 1999b; Desprat et al. 2003; Muñoz Sobrino et al. 2014; Castro et al. 2020; López-Merino et al. 2023). Climate instability is also evident in the Xistral mountains TPD core, where dust events become more frequent after ~4000 cal. yr BP, with several major deposition peaks. Variations in dust flux show a strong climatic signal, likely linked to storminess controlled by North Atlantic Oscillation conditions (Martínez Cortizas et al. 2020). Although climate remained an important driver of landscape change in late Holocene Galicia, increasing anthropogenic pressure became an additional, often dominant, control on vegetation and land dynamics (Muñoz Sobrino et al. 1997; Ramil-Rego et al. 1998; Mighall et al. 2006, 2023; Martínez Cortizas et al. 2009; López-Merino et al. 2012, 2023; Silva-Sánchez et al. 2014). Against this backdrop, the TOX sequence records marked changes in both fen and landscape vegetation (Fig. 6).

A cooling and hydrological deterioration at ~5000-4500 cal. yr BP in the Xistral is corroborated by bog geochemistry, with temperatures up to ~2-2.5 ºC below present (and up to ~5 ºC below the HCO) inferred from mercury variations at PVO (Martínez Cortizas et al. 1999b). In the TOX profile, a sand-rich layer dated to ~4900-4200 cal. yr BP coincides with a shift from the brown peat of Unit III to the black peat of Unit IV, the onset of woodland retreat, and a decline in *Sphagnum* (both percentage and influx), reflected by a drop in the variance explained by PC1 in zone TOX-4a (Fig. 6). Regionally, soil erosion intensified across Galicia: stone-rich layers are reported at multiple sites – e.g., Campo Lameiro colluvial soils (Costa Casáis et al. 2009; Kaal et al. 2011), – and the natural stability of slope soils deteriorated (Martínez Cortizas et al. 2009). Given TOX's valley-floor position, conducive to trapping eroded material, the documented increase in rainfall by 45% from ~4600 to ~4300 cal. yr BP in Galicia (Fábregas Valcarce et al. 2003), together with catchment woodland clearance (Fig. 6) likely combined to enhance runoff and delivered the observed sand input to the fen. This event is not captured in the studied bogs of the Xistral owing to their decoupling from local hydrology, and TOX is the first and only fen analysed in the area, underscoring the sensitivity of fens to catchment-scale processes and their value as environmental archives.

Following this erosive short-term phase, fire activity increased sharply, becoming a major driver of landscape change, coeval with the rising importance of PC2 explaining the variance in zones TOX-4a and TOX-4b (Fig. 6). Both local and regional indicators (CHAR and microcharcoal influx) show an abrupt rise at ~4200 cal. yr BP. Although some authors attribute increased microcharcoal accumulation exclusively to erosion pulses mediated by natural forest fires at ~4250-4150 cal. yr BP (~2300-2200 BC) under colder, drier conditions in NW (Blanco-González et al. 2018), human-mediated fires were also likely significant. This is supported by pedoanthracological evidence from Galician colluvial soils showing rising charcoal content since ~5500 cal. yr BP (Carrión et al. 2010; Kaal et al. 2011, 2013; López-Merino et al. 2012) and by charcoal data from Xistral bogs: TPD from ~4259 cal. yr BP and PDC from ~4620 cal. yr BP (Mighall et al. 2006; Stefanini et al. 2018). The anthropogenic origin of the fires is consistent with palynological evidence of progressive woodland decline and the presence of nitrophilous herbaceous taxa and dung fungi (see Fig. 6 for TOX).

Two main burning phases are detected at TOX: ~4200-3300 cal. yr BP and ~2440-1300 cal. yr BP. Charcoal records from other archives also provide two periods with more intense burning: in TPD at ~4250-3650 cal. yr BP and ~1600-650 cal. yr BP (Stefanini et al. 2018), in PDC at ~4620-3845 cal. yr BP and ~1355-555 cal. yr BP (Mighall et al. 2006), and in BCG at ~4500-4000 cal. yr BP and ~1500-500 cal. yr BP (Souto 2018). In the case of TOX, both phases are characterised by reduced PC1 and increased PC2 or PC3 explaining the variance of the samples, indicating the replacement of the mid-Holocene *Sphagnum*-rich fen by an Ericaceae-rich assemblage and/or wet meadows (Fig. 6). *Calluna vulgaris* and *Erica mackaiana* are more frequent in drier fens than in wet fens, whereas *Sphagnum* shows the opposite pattern. Thus, recurring fire likely lowered peat moisture and favoured Ericaceae during fire-intense phases. The intervening period of reduced charcoal (~3300-2440 cal. yr BP) shows the recovery of *Sphagnum* (Fig. 6). A similar dynamic is evident in PDC, where *Sphagnum* macroremains contribute substantially to the assemblage from ~3100 to ~2200 cal. yr BP but are rare before or after (Castro et al. 2015). By contrast, the bog interval of PVO yielded a chemical signature indicative of dominance by monocots (*Carex durieui*, *Agrostis curtisii*, *Festuca rubra*, *Molinia caerulea*), with intermittent importance by *Eriophorum angustifolium* and minor inputs from other Cyperaceae, Poaceae and *Sphagnum* spp. (Schellekens et al. 2011). However, pollen and/or macroremains from PVO (Muñoz Sobrino et al. 2005) and other Xistral bogs sequences such as PDC and PDC2, BCG (=BLL), and TPD (Mighall et al. 2006, 2023; Castro et al. 2015; Souto 2018; Stefanini et al. 2018) indicate a stronger role for Ericaceae during the last millennia than that inferred from biomarkers alone.

Two major ancient phases of atmospheric metal pollution have been identified in the Xistral bogs: ~3400-2900 cal. yr BP (Bronze Age) and ~2000-1500 cal. yr BP (Roman times) (Martínez Cortizas et al. 2002; Pontevedra-Pombal et al. 2013). It is therefore plausible that fire use for mining-metallurgical activities contributed to burning signals. Human-mediated fires would have opened the landscape for grazing (dung fungi) – particularly during Roman times, when PC3 gains importance (Fig. 6) – and timber may have supplied metallurgical processes. Notably, despite evident fire, woodland clearance, dung fungi and nitrophilous taxa are detected, no major erosion is detected in this interval beyond some scattered presence of *Glomus* cf. *fasciculatum* (HdV-270), implying that heathland and remnant woodlands were sufficient to protect slopes.

In summary, the Late Holocene is characterised by disturbance. Orbital forcing sets a slow trend towards muted seasonality, but human activity becomes the dominant driver of landscape and mire dynamics – intensifying fire, opening the landscape, and suppressing

Sphagnum-rich peat formation. This highlights the importance of considering both climatic variability and human land-use as interacting drivers of biodiversity change in peatland ecosystems.

Today's mire features and threats: Cyperaceae-rich fen and insights for fen conservation in the Xistral Mountains (TOX-5: <~85 cal. yr BP)

Galician peatlands are of outstanding conservation value under the EU Habitats Directive, with Annex I types well represented across the region – blanket bogs, raised bogs, transition mires and fens. These designations underpin Natura 2000 listings and are embedded in Spanish and Galician legislation that mandates protection and guides restoration planning. Beyond their legal status, peatlands are functionally critical: they store carbon at long-term scale, regulate catchment hydrology, and support specialist biota (Silva-Sánchez et al. 2023). Yet many sites – especially fens – are small, fragmented and hydrologically altered, so legal protection alone does not guarantee favourable condition in the field. In the Xistral Mountains, the principal pressures include drainage, commercial forestry (notably conifer and *Eucalyptus* plantations), recurrent burning, overgrazing, nutrient enrichment and linear infrastructure (roads, tracks, windfarms), all of which depress water tables and accelerate degradation (Silva-Sánchez et al. 2023). In this context, Table 1 provides the modern ecological framework needed to interpret the local significance of key pollen types in TOX, particularly those associated with peat-forming vegetation, wet microsites, fen–heath transitions and disturbance-prone communities.

In the TOX record, zone TOX-5 is characterised by a Cyperaceae-rich fen, consistent with PC4 explaining the variance of the samples and with the vegetation surveys that document multiple sedge species as prominent elements of the floristic assemblage (Table 1). However, the fen shows signs of impairment: the dominance of *Enthorhiza* sp. (HdV-527) in PC4 indicates rapid, clay-rich sediment inputs (van Geel et al. 1983), plausibly linked to catchment afforestation, as *Pinus pinaster* also loads highly on this component (Fig. 5). Additional palynological indicators point to intensified human pressure, including further afforestation with *Eucalyptus* (Fig. 6). Conversion of woodland and heathland to pasture and arable land is reflected by increases in fire activity, dung fungi, *Cerealia* t., *Olea*, *Castanea*, and a suite of nitrophilous taxa typically associated with anthropogenic activity (Fig. 6). All this disturbance prevents *Sphagnum* to recover to the levels seen during the HCO. By contrast, PDC bog profile shows *Sphagnum* recovery in macrofossils (Castro et al. 2015), likely because bogs are hydrologically decoupled from catchment erosion, whereas TOX – being a fen – remains exposed to sediment delivery and water-level drawdown. Afforestation further raises water demand along fen margins, promoting peatland drainage (Silva-Sánchez et al. 2023). In general, fens are more vulnerable than bogs because they remain hydrologically coupled to their catchments, making them particularly sensitive to catchment-scale disturbances such as erosion, drainage and land-use change. However, whole-catchment protection is rarely achieved. Current initiatives in the area are removing/controlling pines and *Eucalyptus*, although the latest management plan for the Xistral peatlands considers only raised and blanket bogs, without reference to fens (Laborda-Bartolomé et al. 2024). We therefore recommend phased removal or strict control of forestry within fen catchments, coupled with careful fire and grazing management and hydrological monitoring, to secure long-term recovery.

Biodiversity trends and conservation insights

Rarefaction provides an estimate of taxonomic richness that is independent of variations in pollen counts among samples (Birks and Line 1992) and can be used to explore changes in vegetation heterogeneity and landscape structure through time (Birks et al. 2016). Pollen richness is higher in the basal and upper parts of the TOX sequence, corresponding to the Greenlandian and Meghalayan stages, whereas values remain comparatively stable during the Northgrippian stage (Fig. 6). Higher richness in the basal section likely reflects the ecological transitions associated with mire initiation and terrestrialisation, when wet meadow communities were progressively replaced by fen vegetation. In contrast, the mid-Holocene interval shows relatively stable richness values, consistent with the hydrologically stable *Sphagnum*-rich fen conditions during the HCO, when vegetation composition remained relatively constant. Pollen richness increases again in the uppermost part of the record, coinciding with increasing anthropogenic disturbance and landscape opening, which promoted the coexistence of multiple vegetation types within the pollen source area.

Overall, these results indicate that periods of ecological transition or disturbance tend to be associated with higher palynological richness, whereas long phases of ecosystem stability are characterised by more homogeneous vegetation assemblages. In this context, the mid-Holocene *Sphagnum*-rich fen phase identified at TOX provides a robust ecological reference baseline for biodiversity conservation and ecosystem restoration in minerotrophic peatlands in the Xistral Mountains, representing a period when fen ecosystems operated under stable hydrological conditions and minimal anthropogenic disturbance.

These results highlight the importance of integrating long-term ecosystem trajectories into biodiversity conservation planning. By linking Holocene dynamics and biodiversity trends with present-day degradation, the TOX record provides a robust framework for defining reference conditions, identifying thresholds of change, and guiding restoration strategies in minerotrophic peatlands. However, some limitations should be acknowledged. The temporal resolution (~275 years per sample) constrains the detection of short-term ecological variability. In addition, the absence of a modern pollen–vegetation calibration dataset for the study area limits quantitative interpretation of pollen–vegetation relationships. Accordingly, biodiversity and disturbance patterns are interpreted here at centennial to millennial scales.

Conclusions

- **Peat inception.** The TOX sequence documents mire initiation shortly after the onset of the Holocene: organic-rich mineral accumulation began ~11,100 cal. BP and true peat formation started at ~10,350 cal. yr BP. A terrestrialisation pathway – with floating mats of hydro-hygrophilous plants – drove the transition from wet meadows to a fen system.
- **Regional coherence of early peat inception.** Comparable early Holocene timing across Xistral records (CVM, TPD, PVE, CDL, PDC2) indicates a regionally synchronous peat inception linked to orbital forcing (high summer/low winter insolation) that enhanced seasonality and promoted both woodland expansion and mire initiation.
- **Ecological trajectory during the early Holocene.** Local vegetation shifted from a Poaceae-rich transitional fen to a *Sphagnum*-rich fen as water tables rose and au-

togenic infilling progressed. Principal component analysis tracks this sequence (PC3→PC5(PC2)→PC1), while the landscape evolved from open post-glacial vegetation to expanding deciduous woodlands.
- **Mid-Holocene hydrological stability.** Under the HCO (~8000-5000 cal. yr BP), declining summer and slightly rising winter insolation weakened seasonality and improved effective moisture. TOX records nearly four millennia of *Sphagnum*-rich, hydrologically stable fen, with high and steady OM proxies' values, and slow, steady accumulation rates – a phase of efficient carbon burial.
- **Late-Holocene disturbance regime.** After ~5000-4500 cal. yr BP, climate variability and rising human pressure became the dominant drivers. In TOX, a sand-rich layer (~4900-4200 cal. yr BP), synchronous woodland retreat, and reduced *Sphagnum* presence reflect catchment erosion under increased rainfall and clearance, highlighting fens' sensitivity to hillslope processes. After this initial event, palaeoecological proxies (dung fungi, nitrophilous taxa) and geochemical evidence for Bronze-Age and Roman metal pollution indicate sustained human activity that opened landscapes and altered mire hydrology, often without large erosional responses where heathland and remnant woods buffered slopes.
- **Fire as a vegetation switch.** Late Holocene fire-intense phases coincide with a shift to an Ericaceae-rich fen. Recurrent burning likely lowered peat moisture, suppressing *Sphagnum* and favouring *Calluna/Erica*; a burning pause (~3300-2440 cal. yr BP) allowed partial *Sphagnum* recovery.
- **Present condition and vulnerability.** Modern TOX is a Cyperaceae-rich fen with signals of fire, clay-rich sediment inputs and afforestation pressure (e.g., *Pinus pinaster, Eucalyptus*), and no clear *Sphagnum* recovery. The afforested landscape does not buffer soil-erosion impacts on the fen as effectively as natural forest cover. Compared with bogs, fens are more vulnerable because they remain hydrologically coupled to their catchments.
- **Biodiversity and conservation.** Rarefaction results show comparatively stable palynological richness during the Northgrippian stage, whereas higher richness values during the Greenlandian and Meghalayan stages are associated with phases of ecological transition and disturbance. The mid-Holocene (Northgrippian) record preserves the best developed and longest-lasting stable fen phase at TOX, dominated by *Sphagnum* and characterised by minimal anthropogenic disturbance during the HCO. This phase provides a valuable ecological baseline, indicating that fens thrive under stable, high-water tables and low disturbance, but degrade under catchment erosion, drainage, and fire. Evidence-based management should prioritise catchment-scale measures, including phased removal/control of forestry on peat, hydrological monitoring, and careful fire and grazing management, in order to restore *Sphagnum*-rich conditions and, likely, carbon sequestration capacity.

Collectively, our results show that the Xistral mires are shaped by the interplay of orbital-scale forcing, autogenic processes, and human disturbance, with a pronounced late Holocene transition from climate- to human-dominated controls. This long-term perspective is essential for defining realistic conservation targets and improving the resilience of Atlantic fen ecosystems under ongoing climate and land-use change. Future priorities include systematic surveys of additional fens within this bog-dominated landscape. Such evidence will support more robust, site-specific restoration targets for vulnerable fens in the Xistral Mountains.

Supplementary Information The online version contains supplementary material available at https://doi.org/10.1007/s10531-026-03345-5.

Acknowledgements We are grateful to Professor Rosario G. Gavilán (UCM), Professor Martyn P. Waller (Kingston University London), and Dr Kerry A. Brown (Kingston University London) for their assistance in vegetation surveys and plant identification. We also thank Dr Olalla López-Costas (Universidade de Santiago de Compostela) for her support in selecting the peatland, and Dr Pilar Rodríguez Rojo (Universidad de Castilla-La Mancha), Dr Mar Sobral (Universidade de Santiago de Compostela) and Dr María Losada (Polish Academy of Sciences) for their assistance during the fen core retrieval, Ignacio Alonso Felpete (LEB Herbarium) for accessioning the voucher specimens for this work, and Dr Koldo Trapaga (Universidad Rey Juan Carlos) for his suggestions to improve the age-depth model. This paper is a contribution from AHB's PhD thesis, supervised by LLM (primary supervisor), AMC and SMR. LLM is also deeply grateful to the Spanish public health system for their professionalism and care during her oncological treatment.

Author contributions LLM and AMC conceptualised the study (equal). SMR (lead), AMM, AHB, LLM, and RMU conducted the vegetation surveys. LLM (lead), AHB, and AMM collected the peat core. Sample preparation and laboratory analyses were carried out by AHB (lead), AMM, RMU, LLM, and SMR. LLM (lead), AHB, and AMC led the investigation and data analysis. LLM (lead) and AHB prepared figures. LLM and SMR prepared tables. LLM drafted the first version of the manuscript and conducted the changes towards the revised version. All authors contributed to manuscript writing, editing, and interpretation of the different versions. Funding was acquired by LLM.

Funding Open Access funding provided thanks to the CRUE-CSIC agreement with Springer Nature. This research was supported by the Spanish Ministry of Science and Innovation through the Plan Estatal de Proyectos I+D+I Retos Investigación 2020 (grant PID2020-115580RB-I00) and the Ayudas para Incentivar la Consolidación Investigadora 2022 (CNS2022-135247), and by the Comunidad de Madrid through the Programa de Atracción de Talento, modalidad 1 (grant 2019-T1/AMB-12782), all of them awarded to LLM. AHB was supported by a PhD scholarship (PRE2021-100302), funded by the Spanish Ministry of Science and Innovation and linked to the PID2020-115580RB-I00 project.

Data availability Data collected in this study (palynological data, macrocharcoal and microcharcoal data, CHNS elemental data, CIELab colorimetry results, and numerical analyses) are available at Zenodo: https://doi.org/10.5281/zenodo.19551706

Declarations

Competing interests The authors declare no competing interests.

References

Bennet KD (2025) Psimpoll and pscomb programs for plotting and analysis [WWW Document] Psimpoll and pscomb programs for plotting and analysis. URL http://www.chrono.qub.ac.uk/psimpoll/psimpoll.html (accessed 7.4.25)

Birks HJB, Line JM (1992) The use of rarefaction analysis for estimating palynological richness from quaternary pollen-analytical data. Holocene 2:1–10. https://doi.org/10.1177/095968369200200101

Birks HJB, Felde VA, Bjune AE, Grytnes J-A, Seppä H, Giesecke T (2016) Does pollen-assemblage richness reflect floristic richness? a review of recent developments and future challenges. Rev Palaeobot Palynol 228:1–25. https://doi.org/10.1016/j.revpalbo.2015.12.011

Blaauw M, Christen JA (2011) Flexible paleoclimate age-depth models using an autoregressive gamma process. Bayesian Anal 6:457–474. https://doi.org/10.1214/11-BA618

Blanco-González A, Lillios KT, López-Sáez JA, Drake BL (2018) Cultural demographic and environmental dynamics of the copper and early bronze age in Iberia (3300–1500 BC) towards an interregional multiproxy comparison at the time of the 4.2 ky BP event. J World Prehist 31:1–79. https://doi.org/10.1007/s10963-018-9113-3

Carcaillet C, Bouvier M, Fréchette B, Larouche AC, Richard PJH (2001) Comparison of pollen-slide and sieving methods in lacustrine charcoal analyses for local and regional fire history. Holocene 11:467–476. https://doi.org/10.1191/095968301678302904

Carrión JS, Navarro C, Navarro J, Munuera M (2000) The distribution of cluster pine (*Pinus pinaster*) in Spain as derived from palaeoecological data relationships with phytosociological classification. Holocene 10:243–252. https://doi.org/10.1191/095968300676937462

Carrión Y, Kaal J, López-Sáez JA, López-Merino L, Martínez Cortizas A (2010) Holocene vegetation changes in NW Iberia revealed by anthracological and palynological records from a colluvial soil. Holocene 20:53–66. https://doi.org/10.1177/0959683609348849

Castro D, Souto M, García-Rodeja E, Pontevedra-Pombal X, Fraga MI (2015) Climate change records between the mid- and late Holocene in a peat bog from Serra do Xistral (SW Europe) using plant macrofossils and peat humification analyses. Palaeogeogr Palaeoclimatol Palaeoecol 420:82–95. https://doi.org/10.1016/j.palaeo.2014.12.005

Castro D, Souto M, Fraga MI, García-Rodeja E, Pérez-Díaz S, López Sáez JA, Pontevedra-Pombal X (2020) High-resolution patterns of palaeoenvironmental changes during the little ice age and the medieval climate anomaly in the northwestern Iberian peninsula. GSF 11:1461–1475. https://doi.org/10.1016/j.gsf.2020.05.015

Castro D (2017) Reconstrucción paleoambiental das turbeiras da serra do Xistral mediante análises paleobotánicas (http://purl.org/dc/dcmitype/Text). Universidade de Santiago de Compostela.

Clarke GCS, Jones MR (1977) Plantaginaceae. Rev Palaeobot Palynol 24:129–154. https://doi.org/10.1016/0034-6667(77)90051-3

European Commission (2013) Interpretation manual of european union habitats. version EUR 28

Costa Casáis M, Martínez Cortizas A, Pontevedra Pombal X, Criado Boado F (2009) Analysis of landforms in geoarchaeology campo lameiro NW Iberian peninsula. MDCGI 87:39–52

Desprat S, Sánchez Goñi MF, Loutre M-F (2003) Revealing climatic variability of the last three millennia in northwestern Iberia using pollen influx data. Earth Planet Sci Lett 213:63–78. https://doi.org/10.1016/S0012-821X(03)00292-9

Díaz Varela RA, Filgueiras Silva J, Rodríguez Guitián MA, Ramil Rego P (1997) Evaluación de la viabilidad de las repoblaciones de coníferas en la Serra do Xistral (Galicia, NW Ibérico). II Congreso Forestal Ibérico Sección 02:45–50

FábregasValcarce R, Martínez Cortizas A, Blanco Chao R, Chesworth W (2003) Environmental change and social dynamics in the second third millennium BC in NW Iberia. J Archaeol Sci 30:859–871. https://doi.org/10.1016/S0305-4403(02)00264-9

Faegri K, Iversen J, Kaland PE, Krzywinski K (1989) Textbook of pollen analysis, 4th edn. Blackburn Press, Caldwell, N.J.

Finsinger W, Tinner W, Hu FS (2008) Rapid and accurate estimates of microcharcoal content in pollen slides charcoals from the past: cultural and palaeoenvironmental implications Proceedings of the Third International Anthracological Congress 121–124.

Fraga MI, Romero-Pedreira D, Souto M, Castro D, Sahuquillo E (2008) Assessing the impact of wind farms on the plant diversity of blanket bogs in the Xistral Mountains (NW Spain). Mires Peat 4:1–11. https://doi.org/10.19189/001c.128280

Horák-Terra I, Martínez Cortizas A, da Luz CFP, Rivas López P, Silva AC, Vidal-Torrado P (2015) Holocene climate change in central–eastern Brazil reconstructed using pollen and geochemical records of Pau de Fruta mire (Serra do Espinhaço Meridional, Minas Gerais). Palaeogeogr Palaeoclimatol Palaeoecol 437:117–131. https://doi.org/10.1016/j.palaeo.2015.07.027

Joosten H, de Klerk P (2002) What's in a name? some thoughts on pollen classification identification and nomenclature in quaternary palynology. Rev Palaeobot Palynol 122:29–45. https://doi.org/10.1016/S0034-6667(02)00090-8

Kaal J, Carrión Marco Y, Asouti E, Martín Seijo M, Martínez Cortizas A, Costa Casáis M, CriadoBoado F (2011) Long-term deforestation in NW Spain linking the holocene fire history to vegetation change and human activities. Quat Sci Rev 30:161–175. https://doi.org/10.1016/j.quascirev.2010.10.006

Kaal J, Criado-Boado F, Costa-Casais M, López-Sáez JA, López-Merino L, Mighall T, Carrión Y, Silva Sánchez N, Martínez Cortizas A (2013) Prehistoric land use at an archaeological hot-spot (the rock art park of Campo Lameiro NW Spain) inferred from charcoal synanthropic pollen and non-pollen palynomorph proxies. J Archaeol Sci 40:1518–1527. https://doi.org/10.1016/j.jas.2012.09.024

Kylander ME, Weiss DJ, Martínez Cortizas A, Spiro B, Garcia-Sanchez R, Coles BJ (2005) Refining the pre-industrial atmospheric Pb isotope evolution curve in Europe using an 8000 year old peat core from NW Spain. Earth Planet Sci Lett 240:467–485. https://doi.org/10.1016/j.epsl.2005.09.024

Laborda-Bartolomé RA, Blanco-Arias CA, Lagos Abarzuza L, Cardoso Canastra F, Fagúndez Díaz J, Díaz-Varela ER, Díaz-Varela RA (2024) Plan de Manejo Serra do Xistral. Proyecto RURALtXA Ministerio para la Transición Ecológica y el Reto Demográfico 55 pp. Available at https://ruraltxa.com/publicaciones/

Laskar J, Robutel P, Joutel F, Gastineau M, Correia ACM, Levrard B (2004) A long-term numerical solution for the insolation quantities of the earth. Astron Astrophys 428:261–285. https://doi.org/10.1051/0004-6361:20041335

Liu M, Shen Y, González-Sampériz P, Gil-Romera G, ter Braak CJF, Prentice IC, Harrison SP (2023) Holocene climates of the Iberian Peninsula: pollen-based reconstructions of changes in the west–east gradient of temperature and moisture. Clim past 19:803–834. https://doi.org/10.5194/cp-19-803-2023

López Sáez JA, López Merino L (2005) Precisiones metodológicas acerca de los indicios paleopalinológicos de agricultura en la prehistoria de la península Ibérica. Portvgalia 26:53–64

López-Merino L, Silva Sánchez N, Kaal J, López-Sáez JA, Martínez Cortizas A (2012) Post-disturbance vegetation dynamics during the late Pleistocene and the Holocene an example from NW Iberia. Glob Planet Change 92–93:58–70. https://doi.org/10.1016/j.gloplacha.2012.04.003

López-Merino L, Leroy SAG, Eshel A, Epshtein V, Belmaker R, Bookman R (2016) Using palynology to re-assess the dead sea laminated sediments indeed varves. Quat Sci Rev 140:49–66. https://doi.org/10.1016/j.quascirev.2016.03.024

López-Merino L, Tallón-Armada R, Costa-Casais M, Silva-Sánchez N, López-Sáez JA, Martínez Cortizas A (2023) Palaeoenvironmental framing of the o areal roman saltworks and related anthropogenic activities in north western iberia. Environ Archaeol Press. https://doi.org/10.1080/14614103.2023.2206199

Marret F, O'Keefe J, Osterloff P, Pound M (2021) Applications of non-pollen palynomorphs: from palaeoenvironmental reconstructions to biostratigraphy. Geological Society of London

Martínez Cortizas A, Nóvoa Muñoz JC, Pontevedra Pombal FX, Llana Rodríguez JC, García Rodeja Gayoso E (1997a) Paleocontaminación evidencias de contaminación atmosférica antrópica en Galicia durante los últimos 4000 años. Gallaecia 16:7–22

Martínez Cortizas A, Pontevedra-Pombal X, Muñoz JCN, García-Rodeja E (1997b) Four thousand years of atmospheric Pb Cd and Zn deposition recorded by the ombrotrophic peat bog of Penido Vello (Northwestern Spain). Water Air Soil Pollut 100:387–403. https://doi.org/10.1023/A:1018312223189

Martínez Cortizas A, Pontevedra-Pombal X, García-Rodeja E, Nóvoa-Muñoz JC, Shotyk W (1999b) Mercury in a spanish peat bog archive of climate change and atmospheric metal deposition. Sci 284:939–942. https://doi.org/10.1126/science.284.5416.939

Martínez Cortizas A, García-Rodeja E, Pontevedra Pombal X, Nóvoa Muñoz JC, Weiss D, Cheburkin A (2002) Atmospheric Pb deposition in Spain during the last 4600 years recorded by two ombrotrophic peat bogs and implications for the use of peat as archive. Sci Tot Environ 292:33–44. https://doi.org/10.1016/S0048-9697(02)00031-1

Martínez Cortizas A, Mighall T, Pontevedra Pombal X, Novoa Muñoz JC, Peiteado Varela E, Piñeiro Rebolo R (2005) Linking changes in atmospheric dust deposition, vegetation change and human activities in Northwest Spain during the last 5300 years. Holocene 15:698–706. https://doi.org/10.1191/0959683605hl834rp

Martínez Cortizas A, Biester H, Mighall T, Bindler R (2007) Climate-driven enrichment of pollutants in peatlands. Biogeosciences 4:905–911. https://doi.org/10.5194/bg-4-905-2007

Martínez Cortizas A, Costa-Casais M, López-Sáez JA (2009) Environmental change in NW Iberia between 7000 and 500 cal BC. Quat Int 200:77–89. https://doi.org/10.1016/j.quaint.2008.07.012

Martínez Cortizas A, Peiteado Varela E, Bindler R, Biester H, Cheburkin A (2012) Reconstructing historical Pb and Hg pollution in NW Spain using multiple cores from the Chao de Lamoso bog (Xistral Mountains). Geochim Cosmochim Acta 82:68–78. https://doi.org/10.1016/j.gca.2010.12.025

Martínez Cortizas A, López-Costas O, Orme L, Mighall T, Kylander ME, Bindler R, Gallego Sala Á (2020) Holocene atmospheric dust deposition in NW Spain. Holocene 30:507–518. https://doi.org/10.1177/0959683619875193

Martínez Cortizas A, García Rodeja Gayoso E (2001) Turberas de montaña de Galicia. Centro de Información e Tecnoloxía Ambiental

Martínez Cortizas A, Castillo Rodríguez F, Pérez Alberti A, Valcárcel Díaz M, Blanco Chao R (1999a) Atlas climático de Galicia. Junta de Galicia Xunta de Galicia

Mighall TM, Martínez Cortizas A, Biester H, Turner SE (2006) Proxy climate and vegetation changes during the last five millennia in NW Iberia pollen and non-pollen palynomorph data from two ombrotrophic peat bogs in the North Western Iberian Peninsula. Rev Palaeobot Palynol 141:203–223. https://doi.org/10.1016/j.revpalbo.2006.03.013

Mighall TM, Martínez Cortizas A, Silva-Sánchez N, López-Costas O, López-Merino L (2023) Climate change, fire and human activity drive vegetation change during the last eight millennia in the Xistral Mountains of NW Iberia. Quat 6:5. https://doi.org/10.3390/quat6010005

Moore PD, Webb JA, Collinson ME (1991) Pollen analysis. Blackwell Science Ltd.

Muñoz Sobrino C, Ramil-Rego P, Rodríguez Guitián M (1997) Upland vegetation in the North-West Iberian Peninsula after the last glaciation forest history and deforestation dynamics. Veget Hist Archaebot 6:215–233. https://doi.org/10.1007/BF01370443

Muñoz Sobrino C, Ramil-Rego P, Gómez-Orellana L, Díaz Varela RA (2005) Palynological data on major Holocene climatic events in NW Iberia. Boreas 34:381–400. https://doi.org/10.1111/j.1502-3885.2005.tb01108.x

Muñoz Sobrino C, García-Moreiras I, Castro Y, Martínez Carreño N, de Blas E, Fernández Rodríguez C, Judd A, García-Gil S (2014) Climate and anthropogenic factors influencing an estuarine ecosystem from NW Iberia: new high resolution multiproxy analyses from San Simón Bay (Ría de Vigo). Quat Sci Rev 93:11–33. https://doi.org/10.1016/j.quascirev.2014.03.021

Mursyid H, Ramadhan R, Irawan A, Sadono R, Putra ETS, Suryanto P (2025) A global development and dynamics of peatland restoration: a bibliometric analysis. Ecol Indic 177:113724. https://doi.org/10.1016/j.ecolind.2025.113724

Pontevedra-Pombal X, Rey-Salgueiro L, García-Falcón MS, Martínez-Carballo E, Simal-Gándara J, Martínez-Cortizas A (2012) Pre-industrial accumulation of anthropogenic polycyclic aromatic hydrocarbons found in a blanket bog of the Iberian Peninsula. Environ Res 116:36–43. https://doi.org/10.1016/j.envres.2012.04.015

Pontevedra-Pombal X, Mighall TM, Nóvoa-Muñoz JC, Peiteado-Varela E, Rodríguez-Racedo J, García-Rodeja E, Martínez-Cortizas A (2013) Five thousand years of atmospheric Ni, Zn, As, and Cd deposition recorded in bogs from NW Iberia: prehistoric and historic anthropogenic contributions. J Archaeol Sci 40:764–777. https://doi.org/10.1016/j.jas.2012.07.010

Pontevedra-Pombal X, Castro D, Souto M, Fraga I, Blake WH, Blaauw M, López-Sáez JA, Pérez-Díaz S, Valcárcel M, García-Rodeja E (2019) 10,000 years of climate control over carbon accumulation in an Iberian bog (Southwestern Europe). Geosci Front 10:1521–1533. https://doi.org/10.1016/j.gsf.2018.09.014

Pontevedra-Pombal X, Nóvoa-Muñoz JC, García-Rodeja E, Martínez Cortizas A (2006) Mountain mires from Galicia (NW Spain). In: Peatlands evolution and records of environmental and climate changes, Dev Earthh Surf Proc Elsevier BV.

Punt W, Malotaux M (1984) Cannabaceae, Moraceae and Urticaceae. Rev Palaeobot Palynol 42:23–44. https://doi.org/10.1016/0034-6667(84)90061-7

Ramil Rego P, Aira Rodríguez MJ (1993a) Estudio palinológico de la turbera de Pena Veira (Lugo). Anales Jard Bot Madrid 51:111–122

Ramil Rego P, Aira Rodríguez MJ (1993b) Análisis polínico de la turbera de la Charca do Chan da Cruz (Ferreira do Valadouro, Lugo. N.O. de España). Ecol Mediterr 19:71–78. https://doi.org/10.3406/ecmed.1993.1723

Ramil-Rego P, Aira Rodríguez MJ, Taboada Castro MT (1994) Análisis polínico y sedimentológico de dos turberas en las Sierras septentrionales de Galicia (N.O. de España). R Paléobiol 13:9–28

Ramil-Rego P, Muñoz-Sobrino C, Rodríguez-Guitián M, Gómez-Orellana L (1998) Differences in the vegetation of the North Iberian Peninsula during the last 16,000 years. Plant Ecol 138:41–62. https://doi.org/10.1023/A:1009736432739

Reille M (1992) Pollen et Spores d'Europe et d'Afrique du Nord. Laboratoire de Botanique Historique et Palynologie, CNRS, Marseille, France

Reille M (1995) Pollen et spores d'Europe et d'Afrique du Nord, Supplément 1. Laboratoire de Botanique Historique et Palynologie, CNRS, Marseille, France

Reille M (1998) Pollen et spores d'Europe et d'Afrique du Nord, Supplément 2. Laboratoire de Botanique Historique et Palynologie, CNRS, Marseille, France

Reimer PJ, Austin WEN, Bard E, Bayliss A, Blackwell PG, Ramsey CB, Butzin M, Cheng H, Edwards RL, Friedrich M, Grootes PM, Guilderson TP, Hajdas I, Heaton TJ, Hogg AG, Hughen KA, Kromer B, Manning SW, Muscheler R, Palmer JG, Pearson C, van der Plicht J, Reimer RW, Richards DA, Scott EM, Southon JR, Turney CSM, Wacker L, Adolphi F, Büntgen U, Capano M, Fahrni SM, Fogtmann-Schulz A, Friedrich R, Köhler P, Kudsk S, Miyake F, Olsen J, Reinig F, Sakamoto M, Sookdeo A, Talamo S (2020) The IntCal20 Northern Hemisphere radiocarbon age calibration curve (0–55 cal kBP). Radiocarbon 62:725–757. https://doi.org/10.1017/RDC.2020.41

Renault-Miskovsky J, Girard M, Trouin M (1976) Observations De Quelques Pollens D'oléacées Au Microscope Électronique à Balayage. BullAssoc Fr Étud Quat. https://doi.org/10.3406/quate.1976.1278

Rydin H, Jeglum JK (2013) The biology of peatlands, 2nd edn. Oxfor University Press. https://doi.org/10.1093/acprof:osobl/9780199602995.001.0001

Sanmartín P, Silva-Sánchez N, Martínez-Cortizas A, Prieto B (2015) Usual and unusual CIELAB color parameters for the study of peat organic matter properties tremoal do pedrido bog (NW Spain). J Phys Conf Ser 605:012014. https://doi.org/10.1088/1742-6596/605/1/012014

Santos L, Romani JRV, Jalut G (2000) History of vegetation during the holocene in the courel and queixa sierras galicia northwest iberian peninsula. J Quat Sci 15:621–632

Schellekens J, Buurman P, Fraga I, Martínez-Cortizas A (2011) Holocene vegetation and hydrologic changes inferred from molecular vegetation markers in peat penido vello (Galicia Spain). Palaeogeogr Palaeoclimatol Palaeoecol 299:56–69. https://doi.org/10.1016/j.palaeo.2010.10.034

Silva-Sánchez N, Martínez Cortizas A, López-Merino L (2014) Linking forest cover, soil erosion and mire hydrology to late-Holocene human activity and climate in NW Spain. Holocene 24:714–725. https://doi.org/10.1177/0959683614526934

Silva-Sánchez N, López-Merino L, López-Costas O, Moreno Martín Á, Mighall T, Martínez Cortizas A (2023) Peatlands. In: Núñez-Delgado A, Álvarez-Rodríguez E, Fernández-Calviño D (eds) The environment in Galicia: A book of images: Galician environment through images. Springer International Publishing, Cham, pp 149–178. https://doi.org/10.1007/978-3-031-33114-5_10

Souto M, Castro D, Pontevedra-Pombal X, García-Rodeja E, Fraga MI (2016) Characterisation of Holocene plant macrofossils from North Spanish ombrotrophic mires: vascular plants. Mires Peat 18:11. https://doi.org/10.19189/MaP.2016.OMB.236

Souto M, Castro D, Pontevedra-Pombal X (2017) Characterisation of Holocene plant macrofossils from North Spanish ombrotrophic mires: bryophytes. Mires Peat 19:02. https://doi.org/10.19189/MaP.2016.OMB.263

Souto M (2018) Reconstrucción paleoambiental de turberas del Norte de la Península Ibérica mediante análisis de macrofósiles vegetales y grado de humificación de la turba. Universidade de Santiago de Compostela

Stefanini BS, Oksanen PO, Corcoran JP, Mitchell FJ (2018) Appraising the cohesion of palaeoenvironmental reconstructions in north-west Spain since the mid-Holocene from a high temporal resolution multi-proxy peat record. Holocene 28:681–694. https://doi.org/10.1177/0959683617744258

Stevenson J, Haberle S (2018) Macro charcoal analysis: a modified technique used by the department of archaeology and natural history. Available at http://hdl.handle.net/1885/144170

Stockmarr J (1971) Tables with spores used in absolute pollen analysis. Pollen Spores 13:615–621

Stuiver M, Reimer PJ (1993) Extended 14C data base and revised CALIB 3.0 14C age calibration program. Radiocarbon 35:215–230. https://doi.org/10.1017/S0033822200013904

The Angiosperm Phylogeny Group, Chase MW, Christenhusz MJM, Fay MF, Byng JW, Judd WS, Soltis DE, Mabberley DJ, Sennikov AN, Soltis PS, Stevens PF (2016) An update of the Angiosperm Phylogeny Group classification for the orders and families of flowering plants: APG IV. Bot J Linn Soc 181: 1–20. https://doi.org/10.1111/boj.12385

Turner R, Roberts N, Jones MD (2008) Climatic pacing of Mediterranean fire histories from lake sedimentary microcharcoal. Glob Planet Change 63:317–324. https://doi.org/10.1016/j.gloplacha.2008.07.002

van Smeerdijk DG (1989) A palaeoecological and chemical study of a peat profile from the assendelver polder (The Netherlands). Rev Palaeobot Palynol 58:231–288. https://doi.org/10.1016/0034-6667(89)90088-2

van Geel B, Bos JM, Pals PL (1983) Archaeological and palaeoecological aspects of a medieval house terp in a reclaimed raiseg bog area in North Holland. Ber Rijksd Oudheidkd Bodemonderz 33:419–444

Walker M, Head MJ, Lowe J, Berkelhammer M, BjÖrck S, Cheng H, Cwynar LC, Fisher D, Gkinis V, Long A, Newnham R, Rasmussen SO, Weiss H (2019) Subdividing the Holocene Series/Epoch formalization of stages/ages and subseries/subepochs, and designation of GSSPs and auxiliary stratotypes. J Quat Sci 34:173–186. https://doi.org/10.1002/jqs.3097

Yu ZC (2012) Northern peatland carbon stocks and dynamics: a review. Biogeosci 9:4071–4085. https://doi.org/10.5194/bg-9-4071-2012

Yu Z, Loisel J, Brosseau DP, Beilman DW, Hunt SJ (2010) Global peatland dynamics since the last glacial maximum. Geophys Res Lett 37:L13402. https://doi.org/10.1029/2010GL043584b

Authors and Affiliations

Álvaro Hernando Bartolomé[1] · **Álvaro Moreno Martín**[1] · **Rosina Magaña Ugarte**[1] · **Saúl Manzano**[2,3,4] · **Antonio Martínez Cortizas**[5,6] · **Lourdes López-Merino**[1]

✉ Lourdes López-Merino
lourdelo@ucm.es

[1] ENVIROVEG (grupo UCM 910164), Unidad de Botánica, Departamento de Farmacología, Farmacognosia y Botánica, Facultad de Farmacia, Universidad Complutense de Madrid, Madrid, Spain

[2] Área de Botánica, Departamento de Biodiversidad y Gestión Ambiental, Facultad de Ciencias Biológicas y Ambientales, Universidad de León, León, Spain

[3] Quaternary Palynology Lab, Instituto de Medio Ambiente, Recursos Naturales y Cambio Global, Universidad de León, León, Spain

[4] The Bolus Herbarium, Department of Biological Sciences, University of Cape Town, Cape Town, South Africa

[5] EcoPast (GI-1553), Facultade de Bioloxía, Universidade de Santiago de Compostela, 15782 Santiago de Compostela, Spain

[6] Bolin Centre for Climate Research, Stockholm University, Stockholm, Sweden